

Western Kentucky University
TopSCHOLAR®

Masters Theses & Specialist Projects

Graduate School

5-1-2012

Removal of Heavy Metals Using Modified Limestone Media: Zinc and Cadmium

Keerthy Mandadi

Western Kentucky University, keerthy.mandadi536@topper.wku.edu

Follow this and additional works at: <http://digitalcommons.wku.edu/theses>

 Part of the [Environmental Chemistry Commons](#), and the [Materials Chemistry Commons](#)

Recommended Citation

Mandadi, Keerthy, "Removal of Heavy Metals Using Modified Limestone Media: Zinc and Cadmium" (2012). *Masters Theses & Specialist Projects*. Paper 1170.

<http://digitalcommons.wku.edu/theses/1170>

This Thesis is brought to you for free and open access by TopSCHOLAR®. It has been accepted for inclusion in Masters Theses & Specialist Projects by an authorized administrator of TopSCHOLAR®. For more information, please contact connie.foster@wku.edu.

REMOVAL OF HEAVY METALS FROM DRINKING WATER USING MODIFIED
LIMESTONE MEDIA: ZINC AND CADMIUM

A Thesis
Presented to
The Faculty of the Department of Chemistry
Western Kentucky University
Bowling Green, Kentucky

In Partial Fulfillment
Of the Requirements for the Degree
Master of Science

By
Keerthy Mandadi

May 2012

REMOVAL OF HEAVY METALS FROM DRINKING WATER USING MODIFIED
LIMESTONE MEDIA: ZINC AND CADMIUM

Date Recommended 5-3-2012

Cathleen J. Webb

Dr. Cathleen Webb, Director of Thesis

Bangbo Yan

Dr. Bangbo Yan

Rui Zhang

Dr. Rui Zhang

Michelle C. Doerner 4-june-2012

Dean, Graduate Studies and Research Date

I dedicate this thesis to my family for always being an inspiration to me and who supported and encouraged me the most during my challenging times here at Western Kentucky University. Also, I dedicate this thesis to my research advisor, Dr. Cathleen Webb, for her support and help throughout my research.

ACKNOWLEDGMENTS

I would like to thank many people who made this work possible. I would start with my research advisor, Dr. Cathleen Webb, for her constant support and guidance. Thanks to her for having faith in me and for her timely advice which made this work possible and also for supporting me financially, by offering me a teaching assistantship in all of my semesters and helping me out every time I needed help. I would also like to acknowledge Dr. Bangbo Yan for being a good mentor and giving the right advice in order to accomplish my goals. I would like to express my sincere gratitude and thanks to Pauline Norris for not just helping me with Inductively Coupled Plasma (ICP) at the Advanced Materials Institute (AMI) but also for being kind always and for her valuable suggestions. I thank Mrs. Alicia McDaniel for her support and help in providing the required materials on time and being patient with me. Thanks to Dr. John Andersland for his help with the SEM. I would also like to express my gratitude to the faculty and staff of the Department of Chemistry for their valuable assistance, support, and guidance. I also thank Mrs. Shannon Marble and Ms. Aly Anderson for always helping me and making things easier for me. Big thanks to my research group members and all my dear friends for their support, encouragement and friendship.

I owe my deepest gratitude to my family members who have been a constant source of love, concern, support and strength forever. Nothing was possible without their blessings, support and encouragement throughout this journey. Thanks for always being with me. At last a very special thanks to Graduate Studies, Ogden College and the Department of Chemistry for providing me this opportunity to be a part of Western family.

TABLE OF CONTENTS

List of Figures.....	vi
List of Tables.....	ix
Abstract	xii
Chapter One: Introduction.....	1
Chapter Two: Methods and Instrumentation	14
Chapter Three: Experimental Section	22
Chapter Four: Results and Discussions.....	29
Chapter Five: Conclusions.....	78
Chapter Six: Future work	82
Chapter Seven: Perspective.....	83
Bibliography.....	84

LIST OF FIGURES

Figure 1: Zinc pE-pH diagram.....	5
Figure 2: Cadmium pE-pH diagram	7
Figure 3: Thermoscientific ICAP 6500	16
Figure 4: Burrell Wrist action shaker.....	18
Figure 5: ARL Thermo X-ray Diffractometer.....	20
Figure 6: Accumet basic AB15 pH meter.....	21
Figure 7: Calibration graph for zinc obtained on ICP.....	30
Figure 8: Kinetics studies for zinc with uncoated limestone.....	32
Figure 9: Kinetics studies for zinc with iron-coated limestone.....	34
Figure 10: Batch tests with an initial concentration of 20ppm zinc in various amounts of iron-coated limestone.....	36
Figure 11: Batch experiment for zinc with an initial concentration of 40 ppm zinc in various amounts of iron-coated limestone.....	38
Figure 12: Batch experiment with an initial concentration of 100 ppm zinc..... in various amounts of iron-coated limestone with a contact time of 24 hours.....	40
Figure 13: Effect of pH on zinc removal with an initial concentration of 40ppm zinc solution in 10g of iron-coated limestone.	42

Figure 14: Calibration graph obtained for cadmium on ICP at wavelengths.....	
214.4nm and 226.5nm.....	44
Figure 15: Kinetic studies for cadmium with iron-coated limestone.....	46
Figure 16: Kinetics experiment for cadmium with uncoated limestone	48
Figure 17: Batch test for cadmium with an initial concentration of 20ppb.....	50
Figure 18: Batch test for cadmium with an initial concentration of	
40ppb with 2hrs contact time.....	52
Figure 19: Batch test for cadmium with an initial concentration of	
100ppb with 2hrs contact time.....	54
Figure 20: Batch test for cadmium with an initial concentration of.....	
20ppb with 15min contact time.....	56
Figure 21: Batch test for cadmium with an initial concentration of	
40ppb with 15min contact time.....	58
Figure 22: Batch test for cadmium with an initial concentration of	
100ppb with 15min contact time.....	60
Figure 23: Effect of pH on cadmium removal.....	62
Figure 24: SEM image for uncoated limestone.....	66
Figure 25: Analysis report for SEM image obtained for uncoated limestone.....	67
Figure 26: SEM image for iron-coated limestone.....	68
Figure 27: Analysis report for SEM image obtained for iron-coated limestone.....	69

Figure 28: 350x SEM image for iron-coated limestone treated with zinc solution.....	70
Figure 29: 750x SEM image for iron-coated limestone treated with zinc solution.....	71
Figure 30: Analysis report for SEM image obtained for iron-coated limestone..... treated with zinc.....	71
Figure 31: SEM image for uncoated limestone treated with cadmium.....	73
Figure 32: Analysis report for SEM image obtained for uncoated limestone treated..... with cadmium.....	74
Figure 33: XRD graph comparing peaks of uncoated limestone with calcium..... carbonate.....	76
Figure 34: XRD graph comparing uncoated limestone with iron-coated limestone.....	77

LIST OF TABLES

Table 1: Table for Different chemicals and materials.....14

Table 2: Detection limits for various heavy metals.....17

Table 3: Calibration data obtained for zinc on ICP.....29

Table 4: Kinetics experiment with an initial concentration of 20ppm.....
zinc in 5g of uncoated limestone.....31

Table 5: Kinetics Experiment with an initial concentration of 20ppm.....
zinc in 5g of iron-coated limestone.....33

Table 6: Batch test with an initial concentration of 20ppm zinc solution.....
in various amounts of iron-coated limestone with 24hrs contact time.....35

Table 7: Batch experiment for zinc with an initial concentration of
40ppm in various amounts of iron-coated limestone with 24hrs contact time.37

Table 8: Batch experiment for zinc with an initial concentration of.....
100ppm zinc solution in iron-coated limestone with 24hrs contact time.39

Table 9: Effect of pH on zinc removal with an initial concentration.....
of 40ppm zinc solution in 10g of iron-coated limestone.....41

Table 10: Calibration data obtained for cadmium on ICP.....43

Table 11: Kinetics studies for cadmium with an initial concentration
of 20ppb cadmium solution in 10g of iron-coated limestone.....45

Table 12: Kinetics experiment with an initial concentration of 20ppb.....	
cadmium solution in 10g of uncoated limestone.....	47
Table 13: Batch test for cadmium with an initial concentration	
of 20ppb cadmium solution in 5g, 10g, 10g, 20g and 50g of uncoated.....	
limestone with 2hrs contact time.	49
Table 14: Batch test for cadmium with an initial concentration of.....	
40ppb cadmium solution in 5g, 10g, 10g, 20g and 50g of iron-coated.....	
limestone with 2hrs contact time.....	51
Table 15: Batch test for cadmium with an initial concentration of	
100ppb cadmium solution in 5g, 10g, 10g, 20g and 50g of iron-coated.....	
limestone with 2hrs contact time.	53
Table 16: Batch test for cadmium with an initial concentration of	
20ppb cadmium solution using 0.1g, 0.2g, 0.2g, 0.5g and 1g uncoated.....	
limestone with 15min contact time.....	55
Table 17: Batch test for cadmium with an initial concentration of 40ppb	
cadmium solution in 0.1g, 0.2g, 0.2g, 0.5g and 1g of uncoated.....	
limestone with 15min contact time.....	57
Table 18: Batch test for cadmium with an initial concentration of.....	
100ppb cadmium solution in 0.1g, 0.2g, 0.2g, 0.5g and 1g of uncoated.....	
limestone with 15min contact time.....	59
Table 19: Effect of pH on cadmium removal.....	61
Table 20: pH measurements of various solutions.....	63

Table 21: pH measurements zinc solutions treated with iron-coated limestone.....	64
Table 22: pH measurements of cadmium solutions treated with..... uncoated limestone.....	65
Table 23: Analysis data for SEM image obtained for uncoated limestone.....	67
Table 24: Analysis data for SEM image obtained for iron-coated limestone.....	69
Table 25: Analysis data for SEM image obtained for iron-coated limestone treated with zinc.....	72
Table 26: Analysis data for SEM image obtained for uncoated limestone..... treated with cadmium.....	74

REMOVAL OF HEAVY METALS FROM DRINKING WATER USING MODIFIED
LIMESTONE MEDIA: ZINC AND CADMIUM

Keerthy Mandadi

May 2012

87 Pages

Directed by: Dr. Cathleen Webb, Dr. Bangbo Yan, Dr. Rui Zhang

Department of Chemistry

Western Kentucky University

Heavy metal contamination is a serious concern throughout the world. Increased concentrations in drinking water have many negative impacts on human health.

Limestone is an inexpensive and simple media for removing high concentrations of heavy metals from drinking water supplies. Ferric based media is commonly used to remove zinc, cadmium, lead, arsenic and other heavy metals. The drinking water standards set by the US EPA for cadmium, zinc and arsenic are 0.005 mg/L, 5 mg/L and 0.010 mg/L respectively. Bangladesh, parts of India, China and the United States have high concentrations of arsenic in drinking water. Although many technologies exist for heavy metal removal, most of these are complicated and are associated with high costs making them ineffective and unfavorable to be used in impoverished areas.

We propose a novel method that combines the benefits of limestone with the capacity of ferric media in an iron-coated limestone based material. Samples of water with various concentrations of zinc and cadmium were prepared and batch tests were performed using both uncoated and iron coated limestone and are compared in removal efficiency. Kinetics studies showed that zinc is removed to a maximum level after 24 hours, while cadmium takes only 15 minutes. The effect of pH on removal of heavy metals was also studied. Metals are analyzed using Inductively Coupled Plasma Emission Spectroscopy (ICP-ES). Limestone is readily available and is also easy to coat with iron,

making this material a cost effective and affordable method to be used by developing countries.

Chapter 1

INTRODUCTION

Heavy metal contamination is a serious concern as it has many negative impacts on human health. Heavy metals are the natural components of the earth's crust, rocks and raw mineral ores. Heavy metals such as lead, cadmium, nickel, copper, and their compounds are used in steel industries, batteries, electroplating techniques, paints and pigments (Aziz, 2005). Ground water, which is a major source of drinking water, is contaminated with arsenic and other heavy metals by natural dissolution of minerals and volcanic eruptions as well as human activities, industrial pollution and agricultural pollution. Other anthropogenic sources of heavy metal emissions include waste incinerating plants and fossil fuel burning (Zereini, 2005). Fuel and power industries generate 2.4 million tons of arsenic (As), cadmium (Cd), copper (Cu), mercury (Hg), nickel (Ni), lead (Pb), selenium (Se), vanadium (V), zinc (Zn) annually (Browner, 1997). Arsenic, cadmium, cobalt, nickel, lead, vanadium, zinc and platinum group elements are considered as road specific elements since they are derived from combustion residues, abrasion from tires, brake linings, road pavement and corrosion of galvanized protection barriers (Zereini, 2005). Geochemical conditions are responsible for higher levels of arsenic in ground water (Kim, 2000).

In recent years, arsenic contamination in ground water has been found to be epidemic in ground water in Asian countries like Bangladesh, India and China (Hossain, 2005; Ferguson, 2007). Arsenic poisoning has become a great threat to the millions of people in Bangladesh, where the ground water is in contact with arsenic-rich minerals.

Water arsenic levels $> 50 \mu\text{g/L}$ was associated with children's reduced intellectual function in Arai hazar, Bangladesh (Wasserman, 2004). Higher content of arsenic was found to cause skin, lung, bladder cancers (Le, 2000). Arsenic interferes with cellular activity by inhibiting cellular enzymes thus causing cell death and also causes lactic acidosis and other health problems (Janet, 1997; Stocker, 2003). To protect the public health and environment, the US EPA has set standards for pollutants in the air and drinking water contaminants (Benner, 2004). The drinking water standards for some of the heavy metals like cadmium, arsenic, lead and selenium set by the US-EPA (Environmental Protection Agency) are 0.005mg/L , 0.01mg/L , 0.015mg/L and 0.05mg/L , respectively (Peters, 1999). The secondary maximum contaminant level for zinc in drinking water set by US EPA is 5mg/L . Many methods are used for removal of metals such as granular activated carbon (Gu, 2005), carbonate rich aquifer materials (Romero, 2004), mixed valent iron adsorbents (Mishra and Farrell, 2005), dealginated seaweed waste (Gonzalez, 2001), aragonite shells (Kohler, 2007), nanosorbents (Zhang, 2008) and maghemite (Morin, 2008). Many of these materials are not suitable for the limited resources and rural environment of countries like Bangladesh.

The EPA methods of choice for the elemental analysis of water samples are graphite furnace atomic absorption spectroscopy, inductively coupled plasma emission spectroscopy, X-ray fluorescence spectroscopy and stripping potentiometry (Darwish and Blake, 2001). Immunoassays offer an alternate choice as they can be portable and can be used at contamination sites and require minimum sample treatment (Darwish and Blake, 2001). Other methods for detecting arsenic include fluorescent microplate bioassay by

E.coli, electrochemical techniques and iodine solution method (Tani, 2009; Pal, 2010; Yu, 2010; Yuan, 2010).

Heavy metals such as zinc, iron, manganese, and molybdenum are essential micronutrients for plants, animals and human beings and are required in trace amounts. High concentrations have negative impacts on human health. Other heavy metals such as cadmium, vanadium, arsenic, and mercury do not have known biological uses and are only used for industrial purposes.

Zinc (Zn) is a Group 12 element with atomic number 30. The outer shell electronic configuration is $[\text{Ar}] 3d^{10}4s^2$. It has a melting point of 419°C and the boiling point is 907°C . Zinc is electropositive and has an oxidation state +2. Because of its properties (softness and high charge to radius ratio), it has an important role in biochemistry. It occurs in many minerals but the major ore is *sphalerite*, a form of zinc sulfide (ZnS), which also contains iron and is associated with *galena* (PbS) (Cotton, 1999). Other minerals, from which zinc is extracted, include smithsonite (zinc carbonate), hemimorphite (zinc silicate), wurzite (zinc sulfide) and hydrozincite (zinc carbonate). Compounds such as zinc hydroxide $[\text{Zn}(\text{OH})_2]$ are basic and also amphoteric. It has distorted hexagonal close-packed structures. Zinc reacts with oxygen on heating to form zinc oxide (ZnO).

Zinc is mainly used for galvanization and in the preparation of alloys. It is also used in preparation of some pharmaceuticals, cosmetics and construction materials. Both anthropogenic and natural sources are responsible for zinc contamination in environment. The sources include combustion exhaust (Pierson, 1974; Hildemann, 1991), galvanized

metal parts and railings (Legret, 1999; Barbosa, 1999), tire dust (Dannis, 1974), motor oil and hydraulic fluid, brake linings and cement production (Councell, 2004). From the reservoirs of Chattahoochee River basins in Georgia and Florida, sediment cores were studied by Callender and Rice (Callender, 2000) and showed the zinc concentration is in direct correspondence to the traffic density indicating the zinc source to be tire-wear particles (Councell, 2004). Water samples from the Serine River basin (France) showed the presence of zinc isotopes which were due to anthropogenic contamination (Chem, 2008).

Zinc is essential to maintain a good health but increased concentrations may cause skin irritations, vomiting, nausea and stomach cramps. Even higher concentrations cause liver damage, respiratory disorders and disturb protein metabolism. Some of the industrial activities such as coal combustion, mining and galvanizing steel cause water pollution with zinc which increases the acidity of water. Aquatic organisms may accumulate zinc in their bodies. Zinc polluted soil may affect plants, cattle and can contaminate the ground water. Breakdown of the organic matter is also affected by this as zinc has a negative influence on the activities of earthworms and other microorganisms. The activity of the soil is greatly influenced.

The stability of various zinc species in aqueous system at equilibrium is shown in figure 1. Figure 1 represents the oxidation-reduction potential as a function of pH. The upper broken line represents the oxidizing boundary of water whereas the lower line represents reducing boundary. Drinking water is well oxygenated and has a pH of 6-8 where zinc exists as Zn^{2+} ions. At surface pH of 9-11, $Zn(OH)_2$ is the dominant species

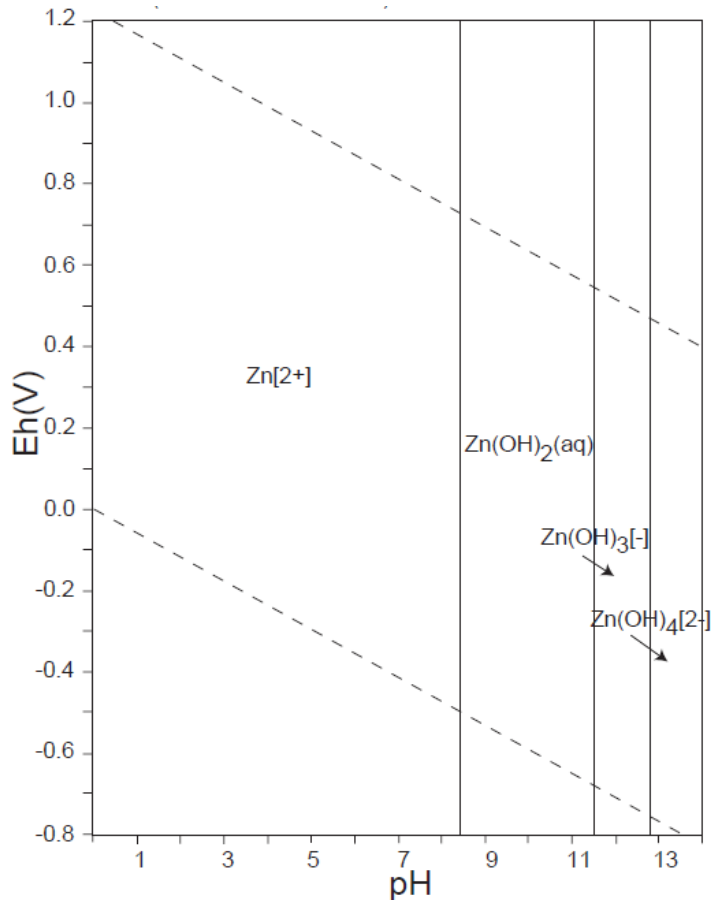


Figure 1: Zinc pE-pH diagram (Brookins, 1988).

Cadmium (Cd) is a transition metal with atomic number 48 and the outer shell configuration is $[Kr] 4d^{10} 5s^2$. It has a melting point of 321°C and the boiling point is 767°C. Cadmium is present in small amounts in most of the zinc ores. Cadmium is also present in some of the lead and copper ores. Some of the rocks mined to produce

phosphate fertilizers also contain large quantities of cadmium. Cadmium does not dissolve in bases but dissolves in simple acids to produce Cd^{2+} ions. Cadmium hydroxide $[\text{Cd}(\text{OH})_2]$ is precipitated by the addition of alkali metal hydroxides. It has a solubility product of 10^{-14} (Cotton, 1999).

Cadmium does not have any biological uses but is widely used for industrial purposes. It is used in electroplating and in the preparation of rechargeable nickel-cadmium batteries. It is also used in photovoltaic cells to convert light energy to electrical energy. Cadmium-helium lasers are a common source of blue-ultraviolet laser light. Cadmium, in the form of cadmium sulfide, is used as a photosensitive material in black and white television phosphors.

Cadmium is released by volcanic activities, metal production, fossil fuel combustion and waste incineration. Industrial processes such as battery production, cement manufacturing, fertilizer production, smelters, iron and steel plants are also sources of cadmium contamination in water and landfills.

Most health and safety agencies identified cadmium and cadmium compounds to be carcinogenic. Cadmium can cause a variety of effects such as nausea, vomiting, diarrhea, muscle cramps, salivation, sensory disturbances, liver injury, convulsions, shock and renal failure. After ingestion or inhalation, cadmium accumulates in the kidney, liver, lungs, and gastrointestinal tract where it causes progressive toxic effects, including cancer and renal damage (Darwish and Blake, 2001).

Cadmium exists as Cd^{2+} ions in the drinking water pH range as shown in figure 2. Cadmium hydroxide $[\text{Cd}(\text{OH})_2]$ is the dominant species at a pH greater than 10.

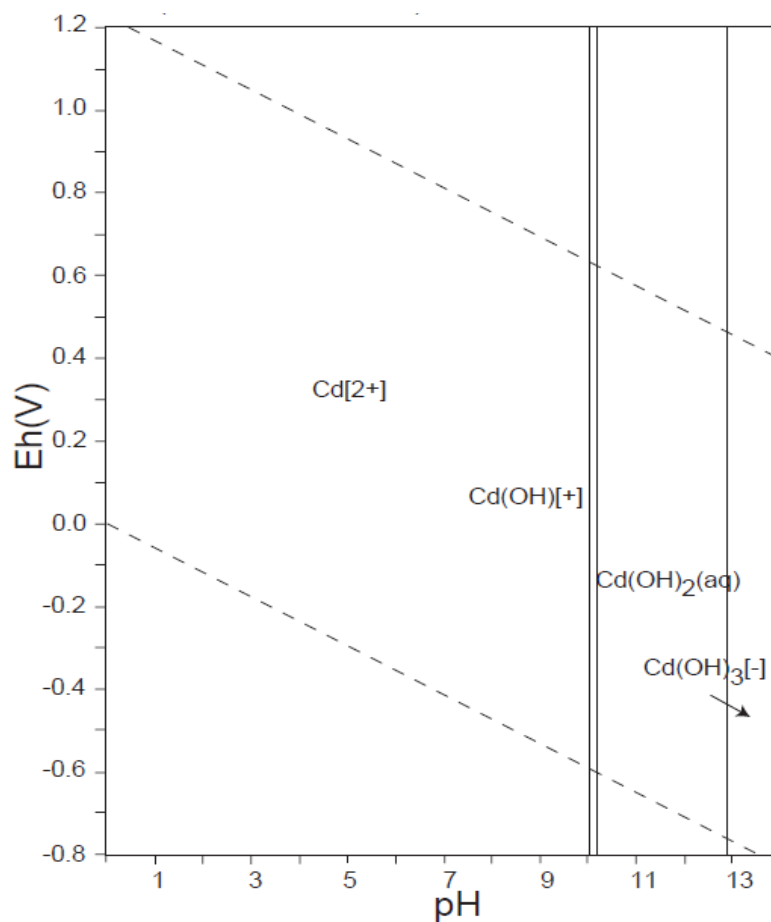


Figure 2: Cadmium pE-pH diagram (Brookins, 1988).

Dealginated seaweed waste (Gonzalez, 2001) was used for the biosorption of cadmium and showed a removal efficiency of 91% in 5 minutes. After 1 hour contact time, the residual cadmium concentration was found to be 0.8mg/L from an initial concentration of 10mg/L. Ion-exchange is the proposed mechanism for removal of the metal. The effect of pH on cadmium biosorption was also observed and showed an optimal cadmium removal at a pH of 6. Other toxic metals like lead (Pb), copper (Cu), nickel (Ni) and chromium (Cr) can also be removed using this sorbent material.

Aragonite shells (Kohler, 2007) were used to remove cadmium from wastewaters where the cadmium metal bearing solutions were treated with shell fragments of various diameters and the uptake of metal crystallites on to the shell surfaces was thought to be through heterogeneous nucleation. Surface precipitation of otavite aided in cadmium removal. The presence of other metals like lead and zinc $\leq 0.3\text{mM}$ does not have any effect on cadmium removal but at higher concentrations lead and zinc compete with cadmium for the carbonate ions which reduces the cadmium removal rates significantly whereas presence of magnesium shows slight enhancement in removal. Zinc and lead were removed faster than cadmium using this method precipitating as $\text{Zn}_5(\text{CO}_3)_2(\text{OH})_6$, PbCO_3 and $\text{Pb}_3(\text{CO}_3)_2(\text{OH})_2$.

In near neutral waters, sphalerite dissolution can be accelerated by the oxidation-reduction reactions involving iron. This was proposed by observing the aqueous metal concentrations and pH of pond water and stream water in contact with high iron sediments. Zinc was observed to undergo partitioning into secondary iron hydroxide and ironoxyhydroxide. Cadmium uptake by calcite takes place only in water with a pH greater than 7 (Carroll, 1998).

Different strains of algae were studied for its uptake capacity for metals like cadmium, zinc, lead and nickel from the aqueous solution through desorption. Lead was removed preferably over the other metals. Phosphorylation of biomass enhanced the binding capacity of *Lyngbya taylorii* with the metals (Klimmek, 2001).

Nanostructured sorbents (Lee, 2005) such as in situ generated agglomerated silica and montmorillonite were also used to capture cadmium species. Suppression of

cadmium nucleation was observed using silica which had a higher surface area and showed a firm binding through chemisorption. Polymeric cation exchanger containing nano-Zr(HPO₃S)₂ is used for the selective sorption of lead, cadmium and zinc (Zhang, 2008).

Previously hydrated lime was used to remove arsenic from the flue gas. Arsenate and arsenite adsorption and desorption behavior on co-precipitated aluminum: iron hydroxides was also studied (Masue, 2007). Other methods proposed for arsenic removal utilized rice husk (Nurul, 2006), hematite, feldspar, aquifer material, schwertmannite and ferrihydrite (Carlson, 2002). A carbonate rich aquifer (Romero, 2004) produces arsenic retention by co-precipitation of complex calcium arsenates or arsenate adsorption onto calcite or clay materials.

Arsenic is released into the drainage and the environment during hard rock mining and leaching of metals and metalloids. Sorption by carbonate rich aquifer material is designed to control the arsenic mobility and retain it during the flow of polluted natural waters. Batch experiments were conducted which showed that 35-90% of soluble arsenic is retained on carbonate rich aquifer material in a pH range of 7-9. Three samples of limestone with minerals hydrous ferric oxides, calcite and a range from hydrous ferric oxides and calcite were used which showed that adsorption and co-precipitation may be the main mechanisms involved in controlling arsenic mobility. In acidic and near neutral solutions hydrous ferric oxides play an important role in arsenic sorption (Romero, 2004).

Research was conducted to determine if Fe (III) containing iron oxides (Yoko, 2007) could produce enough ferric hydroxides to remove minute levels of arsenic in

packed-bed reactors and simultaneously which could prevent bed clogging by avoiding excessive oxide generation. Various column experiments showed the effect of hydraulic detention time, solution pH value, influent arsenic concentration, and concentration of dissolved oxygen on removal efficiency. Arsenic removal rates were higher for media which had higher corrosion rates and removal increased with an increase in the dissolved oxygen levels since Fe^{2+} released by corrosion of media oxidizes at a faster rate.

The primary mechanism involved in arsenic removal by both granular iron oxides and zerovalent iron (ZVI) filings (Dhananjay and James, 2005) is formation of mono-dentate and bi-dentate complexes between arsenic species and ferric hydroxides. Akaganeite and goethite are the granular iron oxide forms generally used to eliminate arsenic in packed bed adsorption systems by many public utilities. In some developing nations, zerovalent iron filings are added to household filters and permeable reactive barriers to remove arsenic. For greater adsorption capacity, an adsorbent should have high porosity, obtained by granulation. Granular ferric hydroxides have slow adsorption kinetics because intra granular diffusion may limit arsenic removal in spite of their rapid complexation with arsenic species. Dissolved oxygen oxidizes Fe^{2+} followed by cationic hydrolysis which generates ferric hydroxides that act as adsorption sites for both As (V) and As (III) compounds.

Granular activated carbon and iron containing adsorbent (As-GAC) (Gu, 2005) was developed for efficient removal of arsenic from drinking water. This method mainly uses granular activated carbon (GAC) as the supporting medium for ferric iron which in turn is charged with ferrous chloride (FeCl_2). With approximately 6% iron content, As-GAC had the highest arsenic removal efficiency but further increases actually reduced

arsenic adsorption. Removal efficiency was observed in a pH range of 4.4-11 but usually reduced above pH 9. Both As (V) and As (III) could be removed to below 10µg/L when groundwater with a concentration of 50µg/L was treated using this method. The important characteristic of activated carbon is its porous structure which gives it a high specific surface area that ranges from hundreds to two thousand m²/g.

The internal pores with specific dimensions act as sites for contaminant adsorption during waste water treatment. The adsorbent abilities were calculated by performing column and batch studies. The adsorption efficiency for arsenic is decreased by 50% with the use of larger sized media. During and after the iron impregnation, the granular nature of activated carbon is conserved and, hence, can be conveniently used for packed-bed applications. “The adsorbent characteristics of GAC were studied using Energy Dispersive Spectroscopy (EDS), Scanning Electron Microscope (SEM), X-Ray Diffraction (XRF) and nitrogen absorption analyses for Brunauer-Emmett-Teller (BET) specific surface area and mesoporous size distribution” (Gu, 2005).

Electrochemical pH adjustment and co-precipitation with iron hydroxide is mainly used to treat acid mine drainage (AMD). The biological oxidation of sulfide materials containing arsenic forms such as arsenite (III) and arsenate As (V) along with large amount of dissolved iron concentrations produce acid mine drainage. By electrochemically reducing H⁺ to elemental hydrogen, pH is raised and arsenic is co-precipitated with iron (III) hydroxide to remove arsenic from synthetic AMD. This is followed by catholyte aeration. Four different AMD model systems were studied. These were Fe (III)/As (V), Fe (III)/As (III), Fe (II)/As (V) and Fe (II)/As (III). Solutions of 300 mg/L of Fe (II), 260mg/L of Fe (III) and 8mg/L of As (V) and As (III) were the initial

concentrations used. Irrespective of the pH adjustment method (done either by adding NaOH or electrochemically), independent results were obtained and all four systems showed quantitative arsenic removal efficiency. Batch tests with Fe (II)/As (V) showed that some elemental iron is deposited on the cathode at higher pH values. When effluent pH is about 4-7, around 85% removal efficiency is observed and the concentrations were reduced to below drinking water standards ($10\mu\text{g/L}$) (Jenny, 2003).

Arsenic uptake by calcite (Alexandratos, 2007) was studied by macroscopic and spectroscopic studies which indicated that uptake mechanism was by both adsorption and co-precipitation. Batch experiments indicated that sorption was rapid in the initial stages and gradually decreased as the sorption sites decreased. Atomic force microscopic studies (Duckworth, 2004) indicate that dissolution and adsorption rates of the adsorbent affects the alkalinity and redox state of natural waters. AFM studies of fluorite removal by calcite again suggest that both adsorption and precipitation occur. Adsorption of fluoride on the surface of calcite and precipitation of fluorite at step edges and kinks where dissolved calcium concentration is highest (Turner, 2005). A highly efficient and low cost technique was developed for the removal of heavy metals using combinations of charcoal and limestone. Coconut carbon can also be used as adsorbent for the removal process (Aziz, 2005). Gravel, limestone, zeolite and cocopeat are used as wetland media and found to enhance the removal rate of arsenic and other heavy metals (Lizama Allende, 2011). Addition of sodium carbonate drop wise to limestone was found to increase the removal rates of heavy metals (Zhigang, 2007).

The main limitations of treatment processes or the technologies such as coagulation/precipitation, membrane separations fluidized bed reactors (Zhou, 1999;

Chen, 2000), biosorption (An, 2001; Gardea, 2004) and ion exchange are that most of them are expensive and are not suitable for small water systems with limited resources. There is an increased necessity to reduce the heavy metal concentrations in drinking water to drinking water standards to protect the consumer from hazardous effects. Limestone is a readily available and inexpensive material which can be used for arsenic and other heavy metal removal such as zinc, cadmium, selenium and lead.

Limestone is a sedimentary rock and is chiefly composed of minerals such as calcite and aragonite. Chemically, limestone is primarily calcium carbonate (CaCO_3). It may contain dolomite ($\text{CaMg}(\text{CO}_3)_2$). Usually limestone has a light or white color but sometimes is tan or grey. Limestone is also seen in different colors because of the impurities such as sand, clay, organic materials, iron oxides and hydroxides. Among sedimentary rocks limestone makes up to 10% of the total. Various types of limestone such as pure limestone, carbonaceous limestone and brecciated limestone were found to have varying degrees of heavy metal removal (Zhigang, 2009). Limestone is pulverized and then sieved so that smaller particles with enhanced surface area are produced (Silva, 2010).

The main purpose of this research is to develop a method to reduce elevated zinc and cadmium concentrations in drinking water to normal US EPA drinking water standards, which is cost-effective, highly efficient, and environmentally friendly with no hazardous waste products and which could be readily applied to real water samples, for both small and large water bodies.

Chapter 2

METHODS AND INSTRUMENTATION

1. Materials and Chemicals

The materials and chemicals used for the research are listed in Table 1.

Table 1: Materials and manufacturers/providers.

Chemical name	Purchased from
Limestone (#16/60)	Pete Lien and Sons, LaPorte, CO
Ferric chloride ($\text{FeCl}_3 \cdot 6\text{H}_2\text{O}$)	Mallinckrodt
Zinc (1000 ppm)	Inorganic Ventures
Cadmium (1000 ppm)	Inorganic Ventures
Whatman cellulose nitrate membrane filters (0.45 μm , 25mm)	Fisher Scientific
Millipore Swinnex Filter Holder	Fischer Scientific
Sodium hydroxide (NaOH) (ACS grade)	Fischer Scientific
Buffers (pH 4 and pH 7)	Fischer Scientific
Nitric acid (Concentrated, Trace metal grade)	Fischer Scientific

2. Inductively Coupled Plasma Emission Spectroscopy (ICP-ES)

Elements dissolved in aqueous or organic liquids can be quantitatively and qualitatively analyzed by inductively coupled plasma spectroscopy. Solid samples may also be digested and analyzed using this system. The excited atoms or ions produced by inductively coupled plasma emit the electromagnetic radiation at wavelengths characteristic of particular elements. Detection of the specific element is based upon the emission of energy at characteristic wavelengths (Skoog, 1998).

Working Principle

It is composed of two parts: Inductively coupled plasma (ICP) and optical spectrometer. Three concentric glass quartz tubes are present in the ICP torch. This quartz torch is surrounded partly by a radiofrequency (RF) generator as can be seen in figure 3. Plasma is created by Argon gas. The radiofrequency signal, which is of high power, flows into the coil. An electromagnetic field is created inside the coil when torch is turned on. The RF generator is a high power radio transmitter that creates the RF signal and drives the “work coil” like a radio transmitter antenna.

The ionization process is initiated as the argon gas flows through the discharge arc. The Tesla unit ignites argon gas that flows through the torch. As the plasma ignites, the Tesla unit is switched off. The ionization of argon gas occurs in the intense electromagnetic field, which flows to the RF coil magnetic field in a rotational symmetrical pattern.

Charged particles collide inelastically with neutral argon atoms and produce stable high temperature plasma of 7000K. Organic or aqueous samples are delivered into a nebulizer by a peristaltic pump. This is converted into mist and directly delivered to the plasma flame. The sample breaks into ions as it collides with charged ions present in the plasma and with that of electrons. Different molecules break into atoms and atomic ions again combine in plasma repeatedly remitting radiation at the characteristic wavelengths of the elements involved. Detection limits are listed in Table 2.

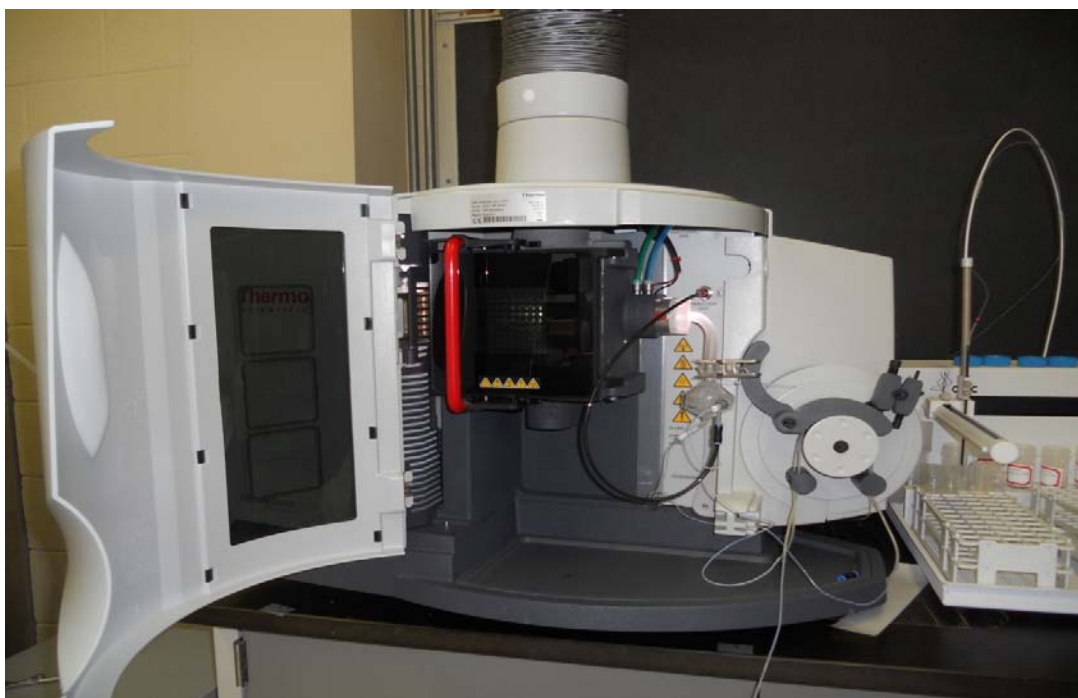


Figure 3: Thermo scientific ICAP 6500

Table 2: Detection limits for various heavy metals.

Metal	$\mu\text{g/L}$
Cadmium	35
Zinc	2.3
Arsenic	1.2
Copper	3.6
Lead	28
Selenium	50

ICP Advantages

- Detection to ppm-ppb levels of numerous trace metals in a sample is possible.
- The important feature of ICP-AES over ICP-AAS is that it is a multi-elemental analysis technique and requires much less time.
- It also requires very low sample volumes.

ICP Disadvantages

- Inert gases and some non-metals such as carbon, nitrogen and oxygen cannot be analyzed by ICP-ES.
- It is an expensive instrument compared to ICP-AAS and is affected by the interferences due to sample preparation and plasma operating conditions.

Applications

- ICP-AES is frequently used for the analysis of trace metals in soil and coal samples.
- It is also used in motor oil analysis and mineral processing.

3. Wrist shaker

The Burrell Wrist action shaker, model 75 shown in figure 4 is used to perform batch tests and to coat the base material. The shaker is constructed in such a way that it may hold conical flasks of 100mL to 1000mL. Flasks that are mounted on a spindle and oscillate through small amplitude shaking. Electronic regulator controls the action of shaking speed.



Figure 4: Burrell Wrist Action Shaker

4. Scanning Electron Microscope (SEM)

Operation

SEM (Scanning Electron Microscopy) has higher resolution in comparison to standard light microscope and used for observing the surface structure of the limestone particles. The JEOL JSM-5400 LV SEM was the used to analyze the samples.

Preparation of Samples for SEM

The samples must be electrically conductive, dry of water and solvents that can vaporize in vacuum and should be firmly mounted. Mounting of the samples for SEM is usually done on metal holders called stubs. The samples are mounted on the stub with the help of a mounting medium. The mounting medium commonly used is glue or tape. The mounting medium should be stable upon production of electrons, should release minimal levels of air or solvents, should not interfere with the image produced in SEM, be mechanically stable and should also have electrical conductivity (Flegler, 1993).

If any of the samples are nonconductive they are usually coated to make the samples electrically conductive. Mostly the nonconductive materials are coated with very thin layers of gold. Depending on nature of sample other methods like air-drying, drying using solvent, vapor fixation, vapor prefixation, freeze drying, and poly-L-lysine procedure may be used.

5. X-ray diffractometer

X-ray diffraction studies determine the arrangement and the spacing of atoms in a crystalline material. Both qualitative and quantitative information about the compounds present in a solid sample can be provided by the x-ray powder diffraction. It is a non-destructive analytical technique that gives information about the chemical composition, crystalline structure and physical properties of materials and thin films. The scattered intensity of an x-ray beam hitting a sample is measured as a function of incident and scattered angle, polarization and wavelength. Each crystalline substance has a unique X-ray diffraction pattern. By comparing the pattern of the unknown with a known

compound, the chemical identity of the material is obtained (Skoog, 1998). The ARL Thermo X-ray diffractometer at the Advanced Materials Institute (AMI) shown in figure 5 was used for the analysis of the samples.



Figure 5: ARL Thermo X-ray diffractometer

6. pH meter

The Accumet basic AB15 pH meter shown in figure 6 is used to measure the pH of the solutions. It consists of a glass electrode connected to an electronic meter that measures and displays the pH reading. Buffer solutions of pH 4 and pH 7 were used to calibrate the instrument.

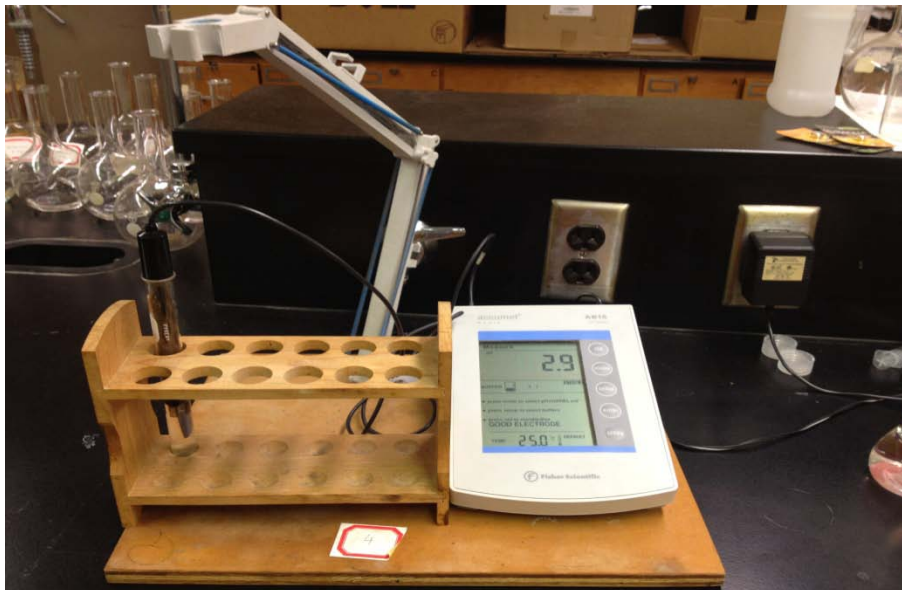


Figure 6: Accumet basic AB15 pH meter

Chapter 3

EXPERIMENTAL SECTION

1. Preparation of working standards

Preparation of 0.1M iron chloride solution:

A sample of 27.00 g of $\text{FeCl}_3 \cdot 6\text{H}_2\text{O}$ was dissolved in 10 mL of nanopure water and transferred to a 1000 mL volumetric flask. The volume is made to 1000 mL with nanopure water.

Preparation of iron-coated limestone:

A sample of 100.00 g of limestone was placed into a round bottom flask. A 100 mL solution of 0.1M iron (III) chloride (FeCl_3) was then placed in the flask. The flask was placed on a shaker. After 24 hours few drops of sodium hydroxide were added to shock the solution, the granules were rinsed with nanopure water and then air dried.

Preparation of 1M sodium hydroxide solution:

A sample of 4.00 g of sodium hydroxide was dissolved in 10 mL of nanopure water which was then transferred to a 100 mL volumetric flask. The volume is made to 100 mL with nanopure water.

Preparation of 20 ppm zinc solution:

An aliquot of 20 mL of 1000 ppm standard zinc solution was placed in a 1000 mL volumetric flask and the volume is made up to 1000 mL with nanopure water.

Preparation of 40 ppm zinc solution:

An aliquot of 40 mL of 1000 ppm standard zinc solution was placed in a 1000 mL volumetric flask and the volume is made up to 1000 mL with nanopure water.

Preparation of 100 ppm zinc solution:

An aliquot of 100 mL of 1000 ppm standard zinc solution was placed in a 1000 mL volumetric flask and the volume is made up to 1000 mL with nanopure water.

Preparation of 100 ppm cadmium solution:

An aliquot of 10 mL of 1000 ppm standard cadmium solution was placed in a 100 mL volumetric flask and the volume is made up to 100 mL with nanopure water.

Preparation of 20 ppb cadmium solution:

An aliquot of 0.2 mL of 100 ppm standard cadmium solution was placed in a 1000 mL volumetric flask and the volume is made up to 1000 mL with nanopure water.

Preparation of 40 ppb cadmium solution:

An aliquot of 0.4 mL of 100 ppm standard cadmium solution was placed in a 1000 mL volumetric flask and the volume is made up to 1000 mL with nanopure water.

Preparation of 100 ppb cadmium solution:

An aliquot of 1.0 mL of 100 ppm standard cadmium solution was placed in a 1000 mL volumetric flask and the volume is made up to 1000 mL with nanopure water.

2. Methods and Experimental Design

Kinetics experiment for zinc with uncoated limestone

A sample of 5 g of uncoated limestone (#16/60) was placed into 10 different 500 mL round bottom flasks and 100 ml of 20 ppm zinc solution was added to each of them. The pH of the 20 ppm zinc standard was measured before being added to the flasks. The

flasks were then placed on a rotary shaker for 0.25, 0.5, 0.75, 1, 1.5, 2, 3, 4, 10 and 24 hours. The speed of the shaker was set to 1-2 cycles/sec. The solution was micro filtered using a 0.45 μ Whatman cellulose nitrate membrane filter and collected into 10 mL vials. The pH was measured and the metal concentration was analyzed by ICP-ES.

Kinetics experiment for zinc with iron-coated limestone

A sample of 5 g of iron-coated limestone (#16/60) was placed into 10 different round bottom flasks and 100 mL of 20 ppm zinc solution was added to each of them. The pH of the 20 ppm zinc standard was measured before being added to the flasks. The flasks were placed on a rotary shaker for 0.25, 0.5, 0.75, 1, 1.5, 2, 3, 4, 10 and 24 hours. The solution was filtered using a 0.45 μ Whatman cellulose nitrate membrane filter and collected into 10 mL vials. The pH was measured and the metal was analyzed on ICP-ES.

Batch tests for zinc

Batch experiment for zinc was performed by adding 5 g, 10 g, 10 g, 20 g and 50 g of iron-coated limestone to five round bottom flasks. To each of these flasks, 100 mL 20 ppm solution of zinc was added and placed on a shaker for 24 hours at a speed of 1-2 cycles/sec. The pH was measured before and after the batch tests. The solutions were then micro filtered and analyzed by ICP-ES for the detection of residual zinc concentrations and iron in the solution. The same procedure was repeated using 40 ppm and 100 ppm zinc standard solutions.

Effect of pH on removal of zinc

This experiment was performed with a 40 ppm zinc solution with 10 g of iron-coated limestone. Initially 10 g of iron-coated limestone was added to seven round bottom flasks. The initial pH of the 20 ppm zinc solution was found to be 2. A volume of

100 mL of 20 ppm zinc solution was added to the first flask. Then the pH of the 20 ppm zinc solution was adjusted to pH 4, 5, 6, 7, 8 and 9 with 1M sodium hydroxide solution. A 100 mL solution of each adjusted pH was added to the other five round bottom flasks. The six flasks were then placed on the rotary shaker for 24 hours at a speed of 1-2 cycles/sec. The solutions were then micro filtered and analyzed by ICP-ES.

Microfiltration

The syringe was rinsed three times to avoid contamination of the sample to be filtered. The sample solution was then filtered through 0.45 μ Whatman cellulose nitrate membrane filters placed on a Swinnex filter holder. The cap on the holder was screwed to the syringe and the solution was then filtered through and collected into a 10 mL vial.

Detection of zinc by ICP-ES

Zinc solutions were analyzed using inductively coupled plasma atomic emission spectroscopy (ICP-ES). The wavelengths used for the detection of zinc are 202.5 nm and 213.8 nm. The samples were also analyzed for the detection of any iron in the solution from the iron-coating on the limestone. Eight calibration standards were prepared – blank, 0.5 ppm, 1 ppm, 2.5 ppm, 3.75 ppm, 5 ppm, 7.5 ppm and 10 ppm standards. All the samples were diluted by a factor of 10 with nano pure water prior to analysis. The sample flush time was set to 80 seconds.

Methods and Experimental Design: Cadmium

Kinetics experiment for cadmium with uncoated limestone

A sample of 10 g of uncoated limestone (#16/60) was placed into 10 different 500 mL round bottom flasks and 100 ml of 20 ppb cadmium solution was added to each of them. The pH of 20 ppb cadmium standard was measured before adding to the flasks. The flasks were then placed on a rotary shaker for 0.25, 0.5, 0.75, 1, 1.5, 2, 3, 4, 10 and 24 hours. The speed of the shaker was set to 1-2 cycles/sec. The solution was micro filtered using a 0.45 μ Whatman cellulose nitrate membrane filter and collected into 10 mL vials. The pH was measured and the metal concentration was analyzed by ICP-ES.

Kinetics experiment for cadmium with iron-coated limestone

A sample of 10 g of iron-coated limestone (#16/60) was placed into 10 different round bottom flasks and 100 mL of 20 ppb cadmium solution was added to each of them. The pH of 20 ppb cadmium standard was measured before adding to the flasks. The flasks were placed on a rotary shaker for 0.25, 0.5, 0.75, 1, 1.5, 2, 3, 4, 10 and 24 hours. The solution was filtered using a 0.45 μ Whatman cellulose nitrate membrane filter and collected into 10 mL vials. The pH was measured and the metal was analyzed on ICP-ES.

Batch tests for cadmium

Batch experiment for cadmium was performed by adding 5 g, 10 g, 10 g, 20 g and 50 g of uncoated limestone to five round bottom flasks. To each of these flasks, 100 mL 20 ppb solution of cadmium was added and placed on a shaker for 2 hours at a speed of 1-2 cycles/sec. The pH was measured before and after the batch tests. The solutions were then micro filtered and analyzed by ICP-ES for the detection of residual cadmium

concentrations and iron in the solution. The same procedure was repeated using 40 ppb and 100 ppb cadmium standard solutions.

A second set of batch experiment was done using 0.1 g, 0.2 g, 0.2 g, 0.5 g and 1 g of uncoated limestone and reducing the contact time to 15minutes. Firstly, 0.1 g, 0.2 g, 0.2 g, 0.5 g and 1 g of uncoated limestone was taken and transferred to 5 round bottom flasks. To each of these flasks, 20 ppb solution of cadmium was added and placed on a shaker for 15minutes at a speed of 1-2. The pH was measured before and after doing the batch tests. The solutions are then micro filtered and analyzed by ICP-ES. The same procedure was repeated using 40 ppb and 100 ppb cadmium standard solution.

Effect of pH on cadmium removal

This experiment was performed with a 40 ppb cadmium solution with 10 g of iron-coated limestone. Initially 10 g of uncoated limestone was added to seven round bottom flasks. The initial pH of 20 ppb zinc solution was found to be 3.6. A volume of 100 mL of 20 ppb cadmium solution was added to the first flask. Then the pH of the 20 ppb cadmium solution was adjusted to pH 4, 5, 6, 7, 8 and 9 with 1M sodium hydroxide solution. A 100 mL solution of each adjusted pH was added to the other five round bottom flasks. The six flasks are then placed on the rotary shaker for 2 hours at a speed of 1-2 cycles/sec. The solutions were then micro filtered and analyzed by ICP-ES.

Detection of cadmium by ICP-AES

Cadmium solutions were analyzed using inductively coupled plasma atomic emission spectroscopy (ICP-ES). The wavelengths used for the detection of zinc are 214.4 nm and 226.5 nm. Seven calibration standards were prepared – blank, 5 ppb, 10

ppb, 25 ppb, 50 ppb, 75 ppb and 100 ppb standards. Full strength samples were ran without any dilution. The sample flush time was set to 100 seconds.

Microscopic Studies

Pictures of plain limestone, iron-coated limestone, iron-coated limestone treated with zinc and uncoated limestone treated with cadmium were taken using scanning electron microscope (SEM).

Chapter 4

RESULTS AND DISCUSSIONS

1. Zinc Results

Zinc samples were analyzed using ICP-ES. The calibration data obtained is shown in Table 3 and Figure 7.

Table 3: Calibration data obtained for zinc on ICP.

Zinc Concentration (ppm)	Signal Intensity (202.5 nm)	Signal Intensity (213.8 nm)
0	127.7	132.8
0.5	8952	9192
1	17530	18130
2.5	43870	45050
3.75	65910	67320
5	86790	88070
10	168000	169000

Figure 7 shows the calibration curve obtained for zinc from ICP-ES at the element wavelengths of 202.5 nm and 213.8 nm. Both lines are linear with R^2 values of 0.996 and 0.998, respectively. The x-axis represents the concentrations of the zinc metal. The y-axis represents signal intensity ratio for the instrument.

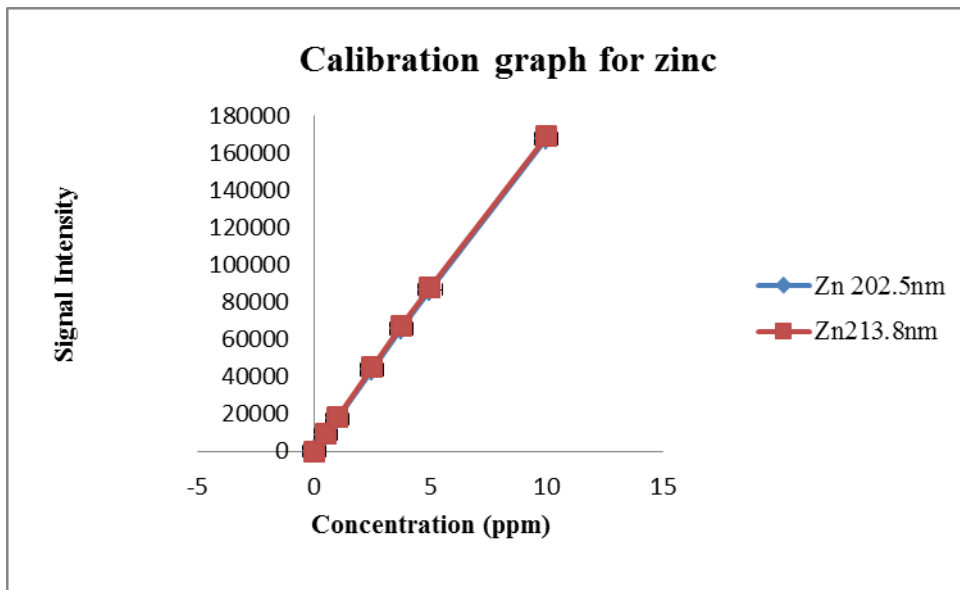


Figure 7: Calibration graph for zinc obtained on ICP

The effectiveness of the method was studied by performing kinetics experiment with iron coated limestone and uncoated limestone. Table 4 and Figure 8 shows the results obtained for kinetics experiment with uncoated limestone.

Table 4: Kinetics experiment with an initial concentration of 20 ppm zinc in 5g of uncoated limestone.

Time (hours)	Concentration of zinc (ppm) (202.5 nm) (± 0.15)	Concentration of zinc (ppm) (213.8 nm) (± 0.15)
0	20.00	20.00
0.25	18.25	18.10
0.5	18.82	16.63
0.75	18.48	16.22
1	18.44	16.12
1.5	16.66	14.66
2	18.89	16.58
3	17.98	17.73
4	19.03	18.77
10	17.9	17.66
24	9.38	8.20

Figure 8 shows a kinetics experiment performed with a fixed initial concentration of 20 ppm zinc solution treated with 5 grams of uncoated limestone for various time intervals. The x-axis represents the time in hours and the y-axis represents the residual concentration of the zinc metal after treatment with plain limestone. The two series represent the concentrations of zinc at wavelengths 202.5 nm and 213.8 nm. It showed the maximum removal after 24 hours. Only about 50% of the metal was removed using plain limestone.

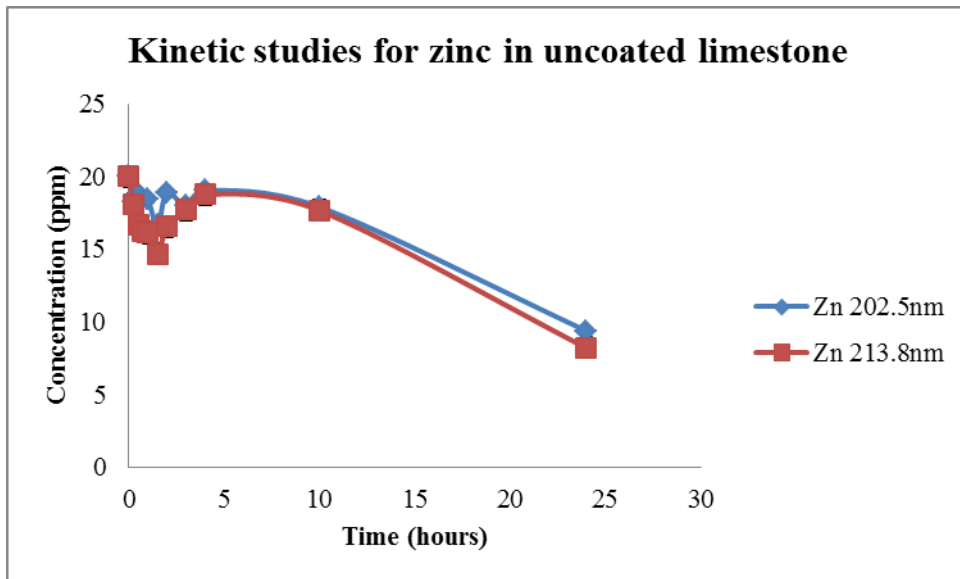


Figure 8: Kinetics studies for zinc with uncoated limestone

The results obtained for kinetics experiment with iron coated limestone are shown in Table 5 and Figure 9.

Table 5: Kinetics Experiment with an initial concentration of 20 ppm zinc in 5 grams of iron-coated limestone.

Time (hours)	Concentration of zinc (ppm) (202.5 nm) (± 0.15)	Concentration of zinc (ppm) (213.8 nm) (± 0.15)
0	20.00	20.00
0.25	3.28	3.14
0.5	10.50	9.95
0.75	11.65	10.94
1	12.36	11.5
1.5	8.88	8.11
2	2.80	2.53
3	1.79	1.61
4	12.95	12.64
10	6.49	5.81
24	1.62	1.43

Figure 9 represents the kinetic studies performed with an initial concentration of 20 ppm zinc solution in contact with 5 grams of iron-coated limestone for various time intervals. The x-axis represents the time in hours and the y-axis represents the zinc metal concentration, post treatment with iron-coated limestone. Zinc metal was found to be reduced in higher amounts with iron coated limestone in comparison to coated limestone. More than 90% of the zinc was removed by 24 hours of treatment with iron-coated limestone. Drinking water standards were met initially at less than 2 hours. The oscillatory results may be due to two removal mechanisms (precipitation as $Zn(OH)_{2(s)}$ and chemisorption through the iron coating).

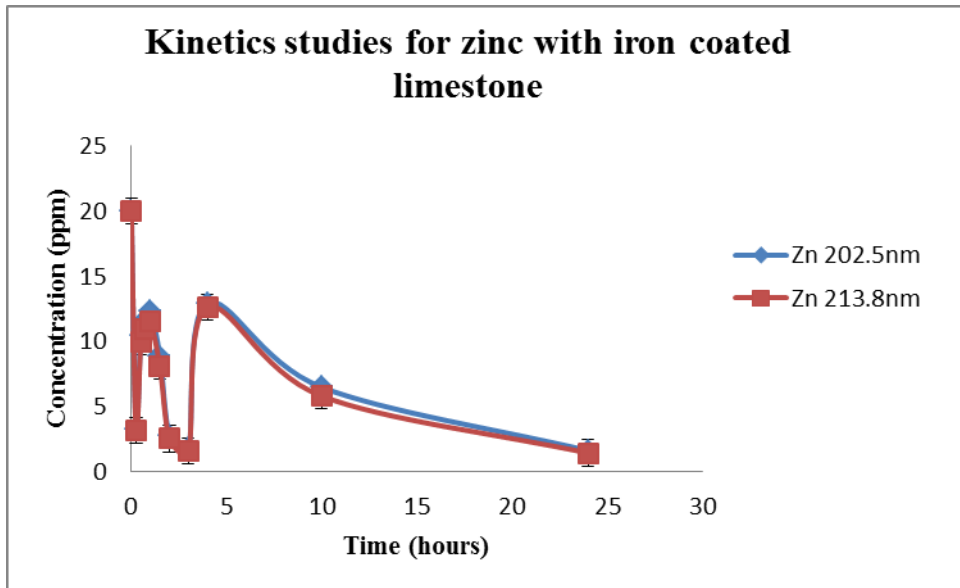


Figure 9: Kinetics studies for zinc with iron-coated limestone

The results obtained for the batch experiment with 20 ppm zinc in iron coated limestone are shown in Table 6 and Figure 10.

Table 6: Batch test with an initial concentration of 20 ppm zinc solution in various amounts of iron-coated limestone with 24 hours contact time.

Weight of iron-coated limestone (grams)	Concentration of zinc (ppm) (202.5 nm) (± 0.15)	Concentration of zinc (ppm) (213.8 nm) (± 0.15)	Concentration of iron (ppm) (240.4 nm) (± 0.15)	Concentration of iron (ppm) (259.9 nm) (± 0.15)	Post treatment pH
0	20.00	20.00	0	0	2.00
5	0.28	0.27	0	0.02	6.40
10	0.45	0.44	0	0.01	6.30
10	0.70	0.68	0.09	0.01	6.50
20	0.26	0.27	0.05	0	6.90
30	0.05	0.06	0	0.01	6.80
50	0.03	0.04	0	0.01	6.80

Figure 10 shows the batch experiment for an initial concentration of 20 ppm zinc solution in various amounts of iron-coated limestone. The x-axis represents the varying weights of iron-coated limestone used and the y-axis represents concentration of zinc for both elemental wavelengths 202.5 nm and 213.8 nm. It also represents the concentration of iron at wavelengths 240.4 nm and 259.9 nm. It was observed that 50 grams of limestone was efficient in reducing 99.8% of metal. The maximum level of iron observed was 0.09 ppm in the solution treated with 10 grams of iron-coated limestone. The drinking standard was met with all weights of iron coated limestone with a reduced zinc concentration to below 5 ppm.

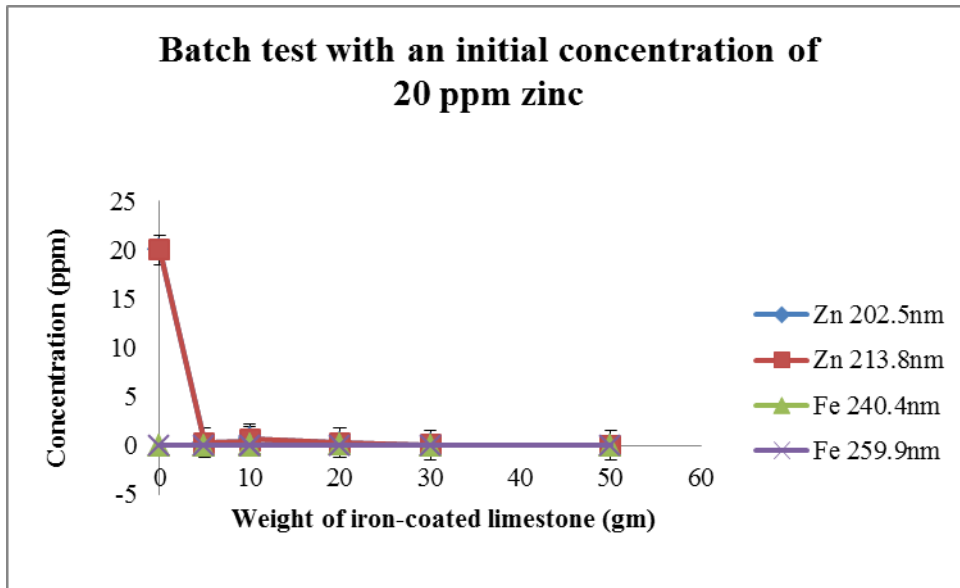


Figure 10: Batch tests with an initial concentration of 20 ppm zinc in various amounts of iron-coated limestone.

The results obtained for the batch experiment with 40 ppm zinc in iron coated limestone are shown in Table 7 and Figure 11.

Table 7: Batch experiment for zinc with an initial concentration of 40 ppm in various amounts of iron-coated limestone with 24 hours contact time.

Weight of iron-coated limestone (grams)	Concentration of zinc (ppm) (202.5 nm) (± 0.15)	Concentration of zinc (ppm) (213.8 nm) (± 0.15)	Concentration of iron (ppm) (240.4 nm) (± 0.15)	Concentration of iron (ppm) (259.9 nm) (± 0.15)	Post treatment pH
0	40.00	40.00	0	0	2.2
5	0.77	0.74	0	0	6.7
10	4.44	4.26	0.01	0.01	6.9
10	5.62	5.38	0	0	7.0
20	4.67	4.45	0	0.03	7.2
50	0.82	0.79	0	0.	7.0

Figure 11 represents the batch experiment with an initial concentration of 40 ppm zinc solution in varying amounts of iron-coated limestone. The x-axis represents the weights of iron-coated limestone used to treat 40 ppm zinc solution. The y-axis represents the residual concentration of zinc after the treatment. About 98% of the metal was removed using 5 grams and 50 grams of limestone. The y-axis also represents the iron concentrations in the treated zinc solutions. The maximum iron concentration was 0.02 ppm present in the solution treated with 20 grams of iron-coated limestone. The drinking water standards were met by all the different weights of iron-coated limestone used.

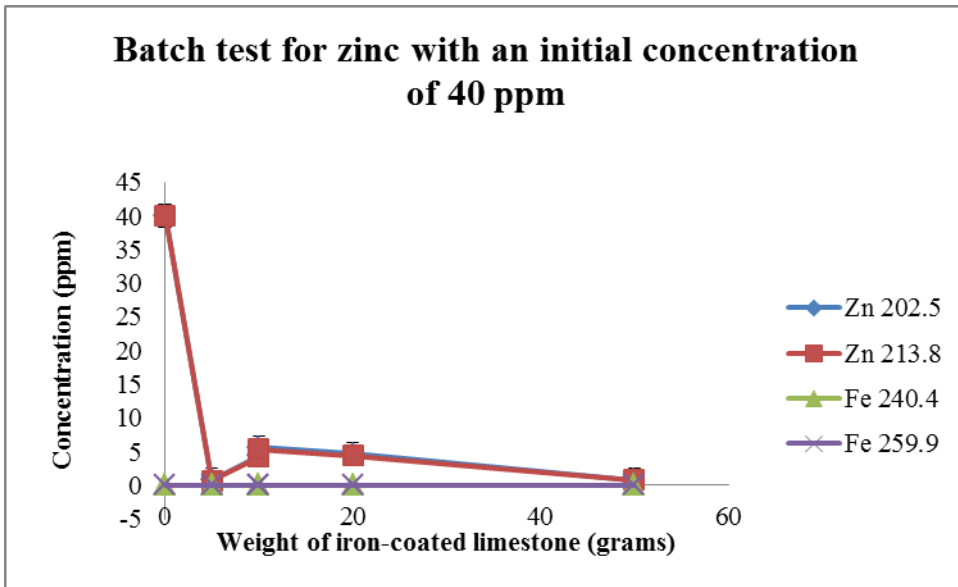


Figure 11: Batch experiment for zinc with an initial concentration of 40 ppm zinc in various amounts of iron-coated limestone.

The results obtained for the batch experiment with 100 ppm zinc in iron coated limestone are shown in Table 8 and Figure 12.

Table 8: Batch experiment for zinc with an initial concentration of 100 ppm zinc solution in iron-coated limestone with 24 hours contact time.

Weight of iron-coated limestone (grams)	Concentration of zinc (ppm) (202.5 nm) (± 0.15)	Concentration of zinc (ppm) (213.8 nm) (± 0.15)	Concentration of iron (ppm) (240.4 nm) (± 0.15)	Concentration of iron (ppm) (259.9 nm) (± 0.15)	Post treatment pH
0	100.00	100.00	0	0	2.0
5	2.56	2.46	0.03	0.02	6.3
10	25.74	24.74	0	0	6.3
10	23.56	23.44	0	0	6.3
20	8.20	7.93	0	0.01	6.2
50	1.30	1.25	0	0	6.2

Figure 12 represents the batch experiment with 100 ppm zinc solution in iron-coated limestone which showed a maximum amount of metal removed at the highest weight of iron-coated limestone used, i.e., 50 grams. The x-axis represents the weights of iron-coated limestone used and y-axis and y-axis represents the concentrations of zinc and iron. The drinking water standards were obtained with 5 grams and 50 grams of iron-coated limestone.

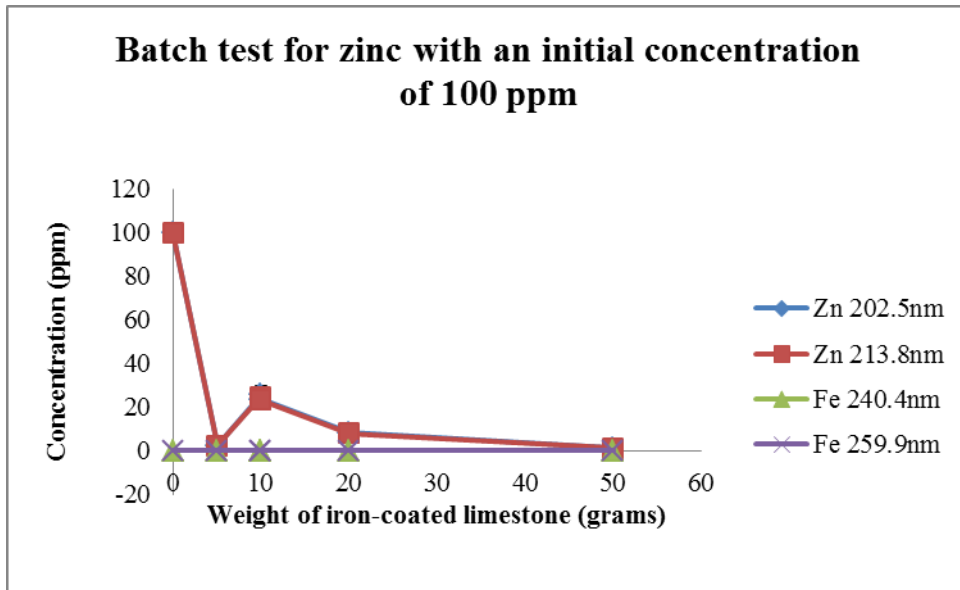


Figure 12: Batch experiment with an initial concentration of 100 ppm zinc in various amounts of iron-coated limestone with a contact time of 24 hours.

The data obtained for the pH experiment with zinc is shown in Table 9 and Figure 13.

Table 9: Effect of pH on zinc removal with an initial concentration of 40 ppm zinc solution in 10 grams of iron-coated limestone.

Initial pH	Percentage removal (%)	Post treatment pH
2	98.27	6.5
4	99.85	7.6
5	99.94	7.6
6	99.96	7.7
7	99.96	7.7
8	99.97	7.8
9	100.00	8

Figure 13 represents effect of pH on zinc removal. The x-axis represents the various pH values of 40 ppm zinc solution before treatment with 10 grams of iron-coated limestone and y-axis represents the percentage removal. It was observed that by increasing the pH of 40 ppm zinc solution from 2 to higher pH removal efficiency was only slightly enhanced. This removal is relatively pH insensitive.

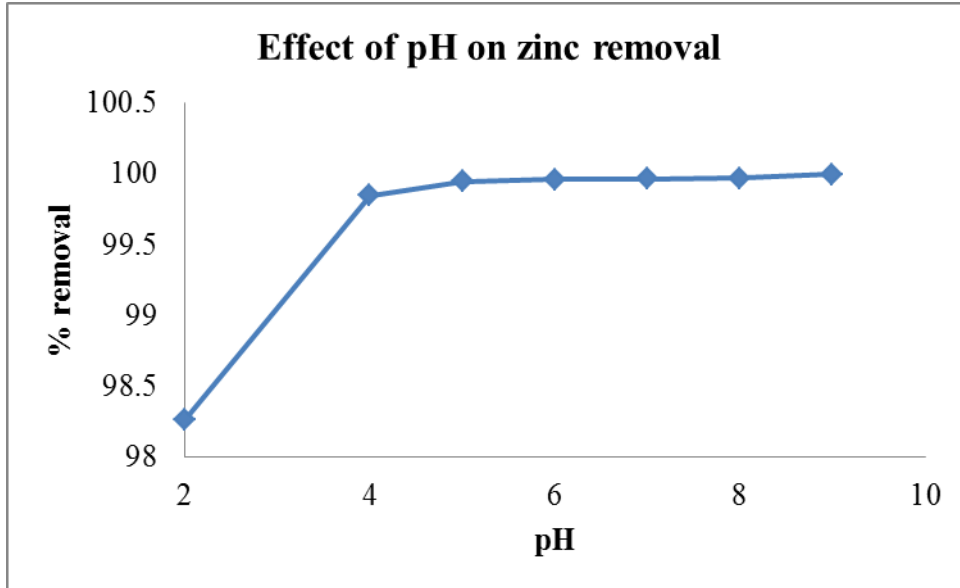


Figure 13: Effect of pH on zinc removal with an initial concentration of 40 ppm zinc solution in 10 grams of iron-coated limestone.

2. Cadmium Results

Cadmium samples were analyzed on ICP-ES. The calibration results obtained are shown in Table 10 and Figure 14.

Table 10: Calibration data obtained for cadmium on ICP.

Concentration (ppb)	Signal intensity (214.438 nm)	Signal intensity (226.502 nm)
0	9.48	5.32
5	122.80	86.04
10	244.70	172.80
25	626.10	446.00
50	1238.00	881.70
75	1848.00	1,319.00
100	2483.00	1,773.00

Figure 14 represents the calibration curve for cadmium obtained at 214.4 nm and 226.5 nm. The x-axis represents the signal intensity and y-axis represents the concentration in ppb. Both the lines were linear with R^2 value of 0.999 and 0.998, respectively.

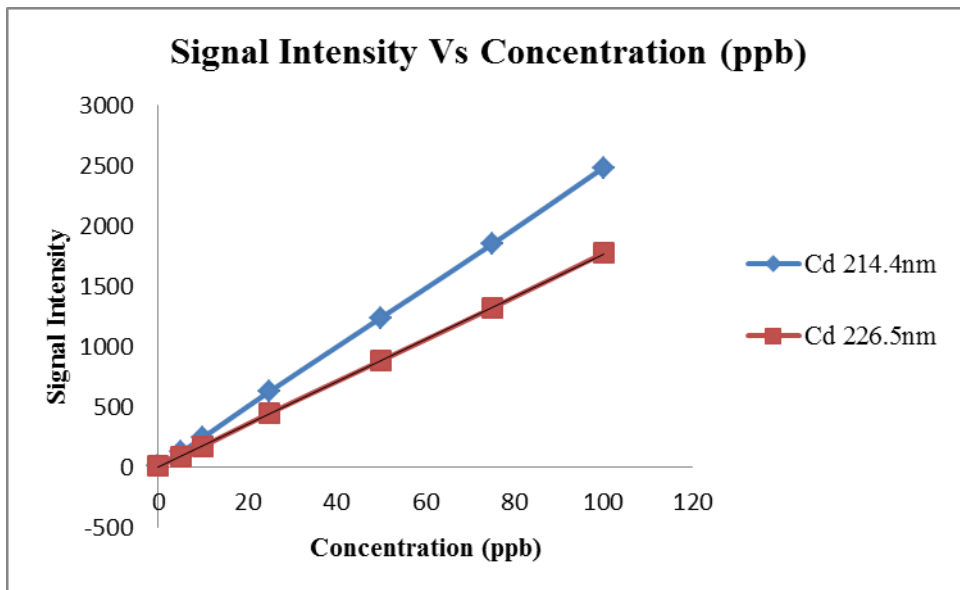


Figure 14: Calibration graph obtained for cadmium on ICP at wavelengths 214.4 nm and 226.5 nm

The efficiency of cadmium removal was studied using kinetics experiments done with both uncoated limestone and iron coated limestone. The results obtained for the kinetics experiment with iron coated limestone are shown in Table 11 and Figure 15.

Table 11: Kinetics studies for cadmium with an initial concentration of 20 ppb cadmium solution in 10 grams of iron-coated limestone.

Time (hours)	Concentration of cadmium (ppb) (214.438 nm) (± 0.15)	Concentration of cadmium (ppb) (226.502 nm) (± 0.15)	Post treatment pH
0.25	ND	ND	7.5
0.50	ND	ND	7.5
0.75	ND	ND	7.6
1.00	ND	ND	7.4
1.50	ND	ND	7.5
2.00	ND	ND	7.1
3.00	ND	ND	7.5
4.00	ND	ND	7.5
10.00	ND	ND	7.5
24.00	ND	ND	7.2

Figure 15 represents the kinetics studies using 20 ppb cadmium solution in 10 grams of iron-coated limestone with varying time intervals. The x-axis represents time in hours and y-axis represents the concentration in ppb. The two wavelengths used are 214.4 nm and 226.5 nm. ICP results showed that the cadmium levels are reduced to zero from an initial concentration of 20 ppb with iron-coated limestone within 15 minutes. The concentration below the drinking water standard of 5 ppb was obtained within 15 minutes with 10 grams of iron coated limestone.

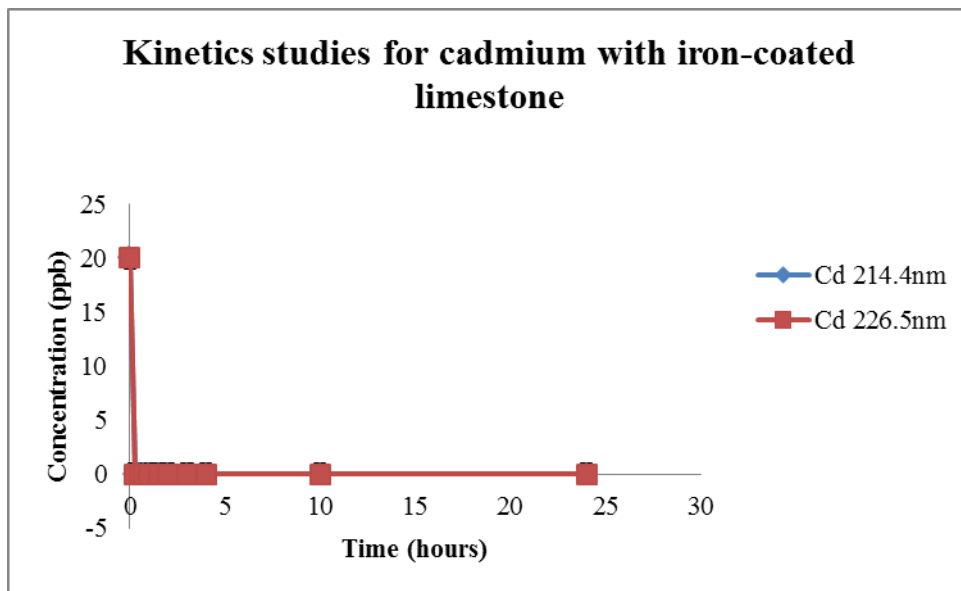


Figure 15: Kinetic studies for cadmium with iron-coated limestone.

The results obtained for the kinetics experiment with uncoated limestone are shown in Table 12 and Figure 16.

Table 12: Kinetics experiment with an initial concentration of 20 ppb cadmium solution in 10 grams of uncoated limestone.

Time (hours)	Concentration of cadmium (ppb) (214.438 nm) (± 0.15)	Concentration of cadmium (ppb) (226.502 nm) (± 0.15)	Post treatment pH
0.25	ND	ND	8.1
0.50	ND	ND	8.1
0.75	ND	ND	8.1
1.00	ND	ND	7.9
1.50	ND	ND	8.1
2.00	ND	ND	8.0
3.00	ND	ND	7.9
4.00	ND	ND	8.0
10.00	ND	ND	7.9
24.00	ND	ND	7.1

Figure 16 represents the kinetics studies using 20 ppb cadmium solution in 10 grams of uncoated limestone. The x-axis represents time in hours and y-axis represents the concentration in ppb. The two wavelengths used are 214.4 nm and 226.5 nm. ICP results showed that the cadmium levels are reduced to zero with uncoated limestone within 15 minutes. All the concentrations were reduced to below drinking water standard of 5 ppb cadmium.

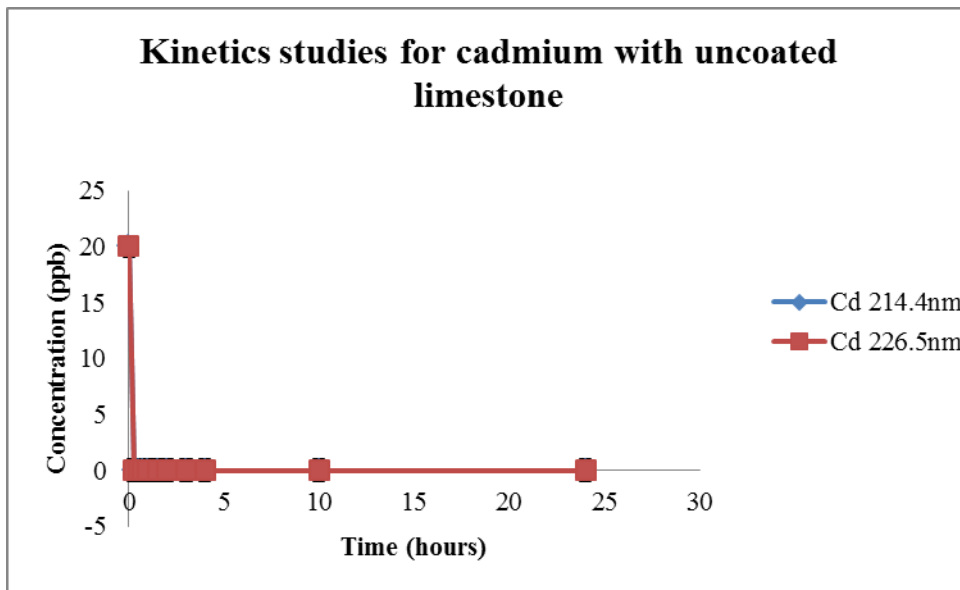


Figure 16: Kinetics experiment for cadmium with uncoated limestone

Batch experiments were done to investigate the removal efficiency with varying amounts of limestone. The results obtained for the first batch experiment with 20 ppb cadmium in uncoated limestone are shown in Table 13 and Figure 17.

Table 13: Batch test for cadmium with an initial concentration of 20 ppb cadmium solution in 5 grams, 10 grams, 10 grams, 20 grams and 50 grams of uncoated limestone with 2 hours contact time.

Weight of uncoated limestone (grams)	Concentration of cadmium (ppb) (214.438 nm) (± 0.15)	Concentration of cadmium (ppb) (226.502 nm) (± 0.15)	Post treatment pH
0	20	20	3.3
5	ND	ND	7.8
10	ND	ND	7.9
10	ND	ND	7.9
20	ND	ND	7.9
50	ND	ND	8.0

Figure 17 represents the batch experiment for 20 ppb cadmium solution treated with 5, 10, 10, 20 and 50 grams of uncoated limestone for 2 hours. The x-axis represents the weight of uncoated limestone and y-axis represents the post treatment cadmium concentration in ppb. ICP-ES results showed that the residual cadmium concentrations were below the detection drinking water standard of 5 ppb.

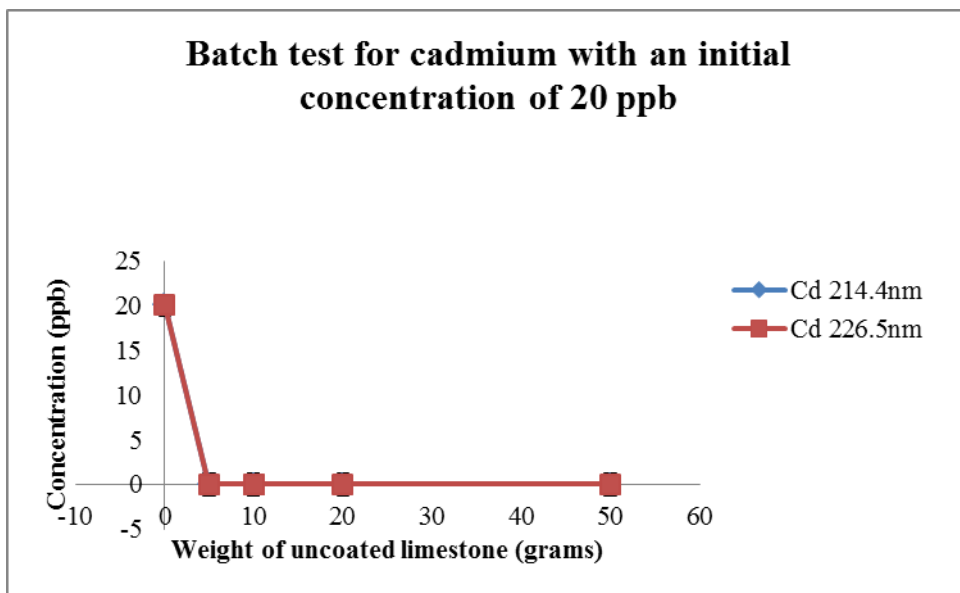


Figure 17: Batch test for cadmium with an initial concentration of 20 ppb.

The results obtained for the first batch experiment with 40 ppb cadmium in uncoated limestone are shown in Table 14 and Figure 18.

Table 14: Batch test for cadmium with an initial concentration of 40 ppb cadmium solution in 5, 10, 10, 20 and 50 grams of iron-coated limestone with 2 hours contact time.

Weight of uncoated limestone (grams)	Concentration of cadmium (ppb) (214.438 nm) (± 0.15)	Concentration of cadmium (ppb) (226.502 nm) (± 0.15)	Post treatment pH
5	ND	ND	8.0
10	ND	ND	8.2
10	ND	ND	8.4
20	ND	ND	8.4
50	ND	ND	8.4

Figure 18 represents the batch experiment for 40 ppb cadmium solution treated with 5, 10, 20 and 50 grams of uncoated limestone for 2 hours. The x-axis represents the weight of uncoated limestone and y-axis represents the post treatment cadmium concentration in ppb. No residual cadmium concentrations were detected post treatment with uncoated limestone. The drinking water standards were obtained with all the weights used.

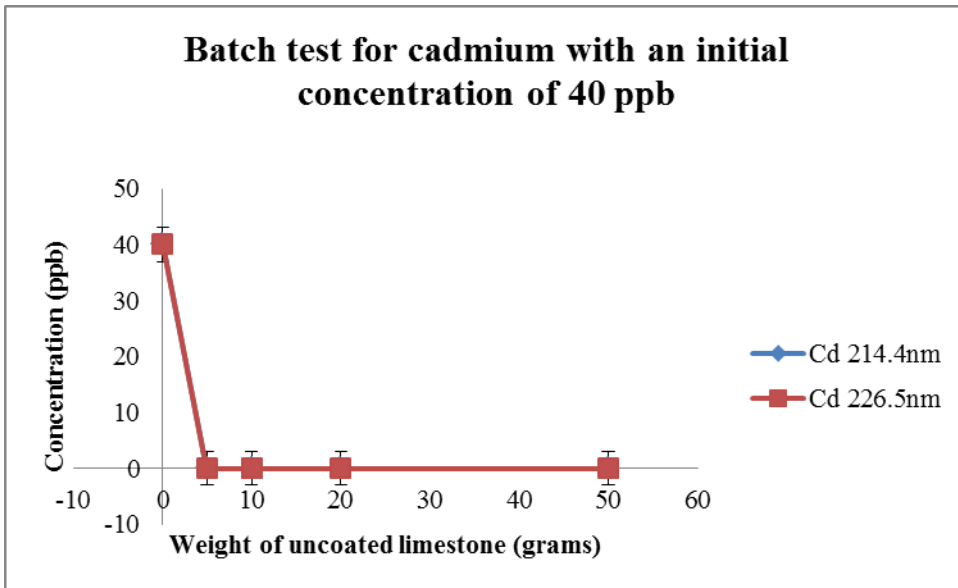


Figure 18: Batch test for cadmium with an initial concentration of 40 ppb with 2 hours contact time.

The results obtained for the first batch experiment with 100 ppb cadmium in uncoated limestone are shown in Table 15 and Figure 19.

Table 15: Batch test for cadmium with an initial concentration of 100 ppb cadmium solution in 5, 10, 10, 20 and 50 grams of iron-coated limestone with 2 hours contact time.

Weight of uncoated limestone (grams)	Concentration of cadmium (ppb) (214.438 nm) (± 0.15)	Concentration of cadmium (ppb) (226.502 nm) (± 0.15)	Post treatment pH
5	ND	ND	7.8
10	ND	ND	7.9
10	ND	ND	7.9
20	ND	ND	8.0
50	ND	ND	8.2

Figure 19 represents the batch experiment for 100 ppb cadmium solution treated with 5, 10, 20 and 50 grams of uncoated limestone for 2 hours. The x-axis represents the weight of uncoated limestone and y-axis represents the post treatment cadmium concentration in ppb. The cadmium concentrations in the solution were below the detection limits indicating 100% removal efficiency of uncoated limestone for cadmium.

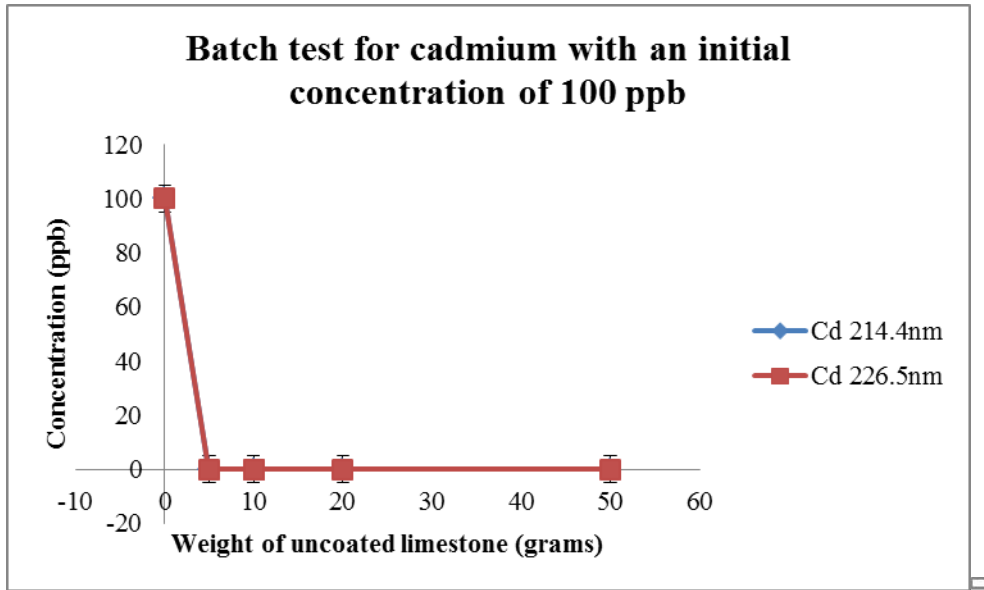


Figure 19: Batch test for cadmium with an initial concentration of 100 ppb with 2 hours contact time.

Since the results obtained from the first batch experiments showed the cadmium removal completely within 2 hours with just 5 grams of uncoated limestone for all the concentrations, a second batch experiment was performed by using weights less than 1 gram and 15 minutes contact time. The results for the second batch experiment with 20 ppb cadmium are shown in Table 16 and Figure 20.

Table 16: Batch test for cadmium with an initial concentration of 20 ppb cadmium solution using 0.1, 0.2, 0.2, 0.5 and 1 gram uncoated limestone with 15 minutes contact time.

Weight of uncoated limestone (grams)	Concentration of cadmium (ppb) (214.438 nm) (± 0.15)	Concentration of cadmium (ppb) (226.502 nm) (± 0.15)	Post treatment pH
0.1	ND	0.03	6.5
0.2	0.06	0.02	7.1
0.2	0.23	0.13	7.0
0.5	0.31	0.28	7.5
1.0	0.23	0.17	7.6

Figure 20 represents the batch experiment for 20 ppb cadmium solution in 0.1, 0.2, 0.2, 0.5 and 1 gram of uncoated limestone with a contact time of 15 minutes. The 99% removal efficiency was observed with 0.2 gram but the concentration slightly increased for 0.5 and 1 gram of uncoated limestone. Though 100 % efficiency was not seen all the concentrations, were reduced to below drinking standard of 5 ppb cadmium.

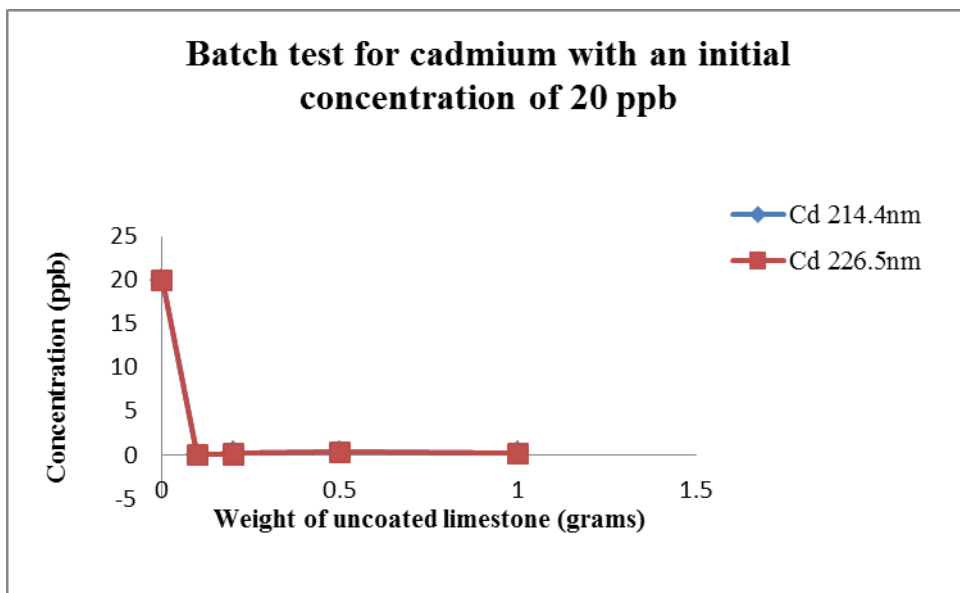


Figure 20: Batch test for cadmium with an initial concentration of 20 ppb with 15 minutes contact time.

The results for the second set of batch experiment with 40 ppb cadmium are shown in Table 17 and Figure 21.

Table 17: Batch test for cadmium with an initial concentration of 40 ppb cadmium solution in 0.1, 0.2, 0.2, 0.5 and 1 gram of uncoated limestone with 15 minutes contact time.

Weight of uncoated limestone (grams)	Concentration of cadmium (ppb) (214.438 nm) (± 0.15)	Concentration of cadmium (ppb) (226.502 nm) (± 0.15)	Post treatment pH
0.1	0.51	0.53	6.5
0.2	0.87	0.92	6.2
0.2	1.77	1.76	6.6
0.5	2.25	2.21	7.5
1.0	1.72	1.73	7.8

Figure 21 represents the batch experiment for 40 ppb cadmium solution in 0.1, 0.2, 0.2, 0.5 grams and 1 gram of uncoated limestone with a contact time of 15 minutes. Only 95.7% removal efficiency was observed with 1 gram whereas 0.1grams removed 98.7% of the metal. All the weights used reduced the concentration to below the drinking water standard of 5 ppb cadmium.

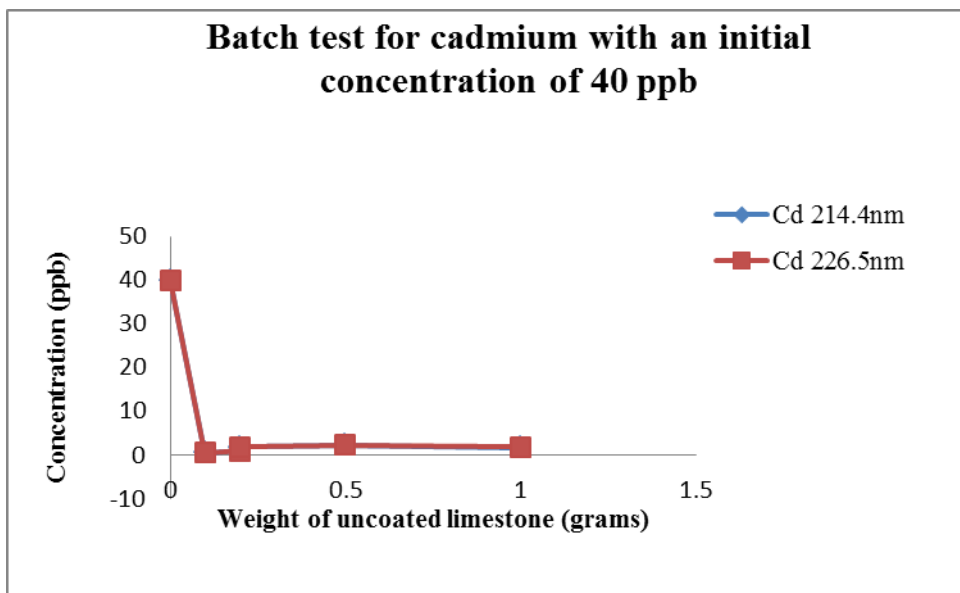


Figure 21: Batch test for cadmium with an initial concentration of 40 ppb with 15 minutes contact time.

The results for the second set of batch experiment with 100 ppb cadmium are shown in Table 18 and Figure 22.

Table 18: Batch test for cadmium with an initial concentration of 100 ppb cadmium solution in 0.1, 0.2, 0.2, 0.5 grams and 1 gram of uncoated limestone with 15 minutes contact time.

Weight of uncoated limestone (grams)	Concentration of cadmium (ppb) (214.438 nm) (± 0.15)	Concentration of cadmium (ppb) (226.502 nm) (± 0.15)	Post treatment pH
0.1	2.84	2.80	6.1
0.2	5.60	5.57	6.5
0.2	7.49	7.37	6.2
0.5	11.54	11.38	6.9
1.0	9.29	9.22	7.3

Figure 22 represents the batch experiment for 100 ppb cadmium solution in 0.1, 0.2, 0.2, 0.5 grams and 1 gram of uncoated limestone with a contact time of 15 minutes. The highest removal efficiency was seen for 0.1 grams which removed about 97% of the metal. The drinking standards were obtained with 0.1, 0.2 grams and 1 gram.

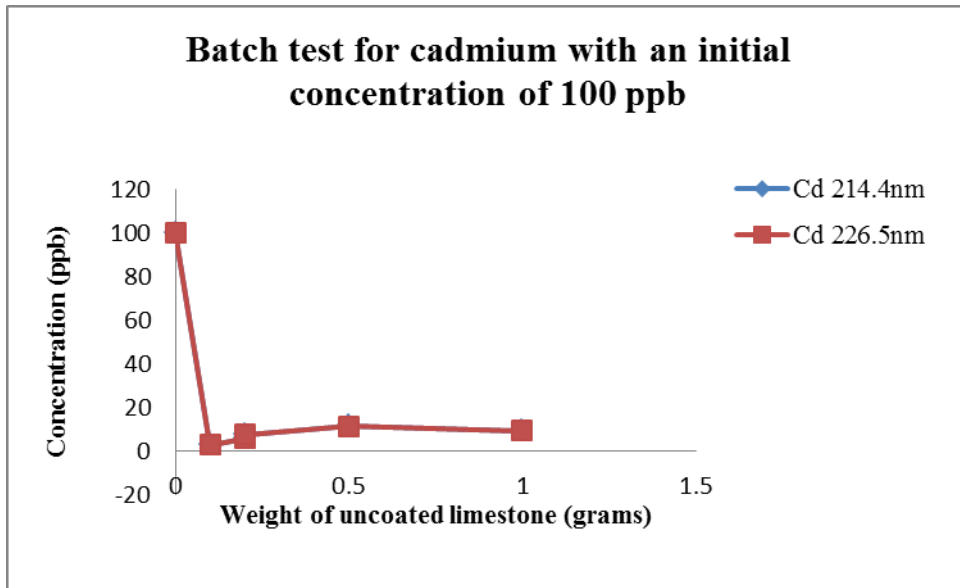


Figure 22: Batch test for cadmium with an initial concentration of 100 ppb with 15 minutes contact time.

The results obtained for the pH experiment with 40 ppb cadmium in 10 grams of uncoated limestone are shown in Table 19 and Figure 23.

Table 19: Effect of pH on cadmium removal

Initial pH	Percentage removal (%)	Post treatment pH
3.6	100	8.3
4.0	100	8.4
5.0	100	8.6
6.0	100	8.8
7.0	100	8.6
8.0	99.11	8.8
9.0	100	9.2

Figure 23 represents the effect of pH on cadmium removal with a fixed concentration of 40 ppb in 10 grams of uncoated limestone. The x-axis represents the pH of 40 ppb cadmium solution before treating with 10 grams of uncoated limestone. The y-axis represents the residual cadmium concentration after treatment with uncoated limestone. ICP-ES results showed the concentration to be below the detection limits indicating pH independence of uncoated limestone for cadmium removal.

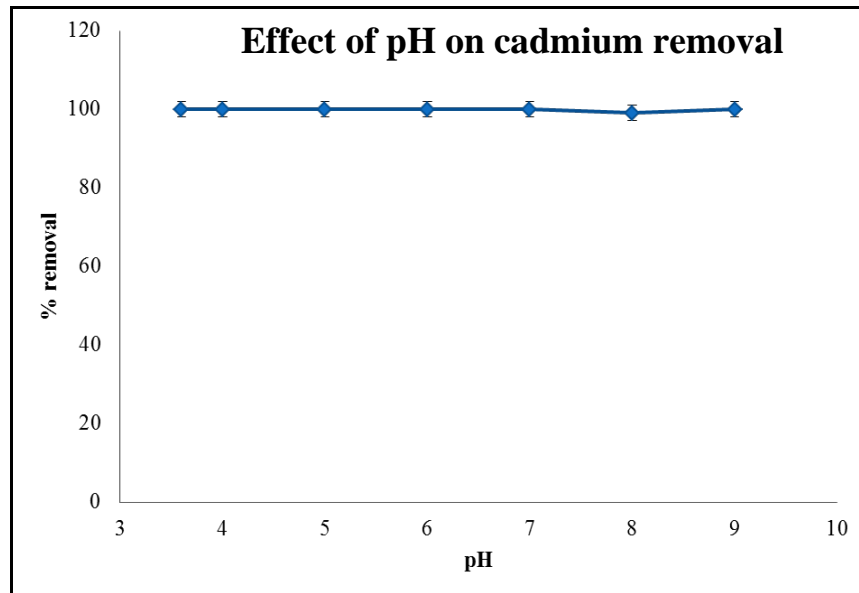


Figure 23: Effect of pH on cadmium removal

The pH values of various solutions measured using pH meter are listed in Table 20. The initial pH values obtained before treating with the base material were acidic for all the solutions.

Table 20: pH measurements of various solutions.

Sample	pH
0.1M Ferric chloride solution	1.6
20 ppm Zinc	2.0
40 ppm Zinc	2.2
100 ppm Zinc	2.0
20 ppb Cadmium	3.3
40 ppb Cadmium	3.6
100 ppb Cadmium	3.2

The pH values of pre and post treated zinc and cadmium solutions are listed in Table 21 and 22, respectively.

Table 21: pH measurements zinc solutions treated with iron-coated limestone.

Weight of iron-coated limestone used (grams)	Post treatment pH		
	20 ppm Zinc	40 ppm Zinc	100 ppm Zinc
5	6.4	6.7	6.3
10	6.3	6.9	6.3
10	6.5	7.0	6.3
20	6.9	7.2	6.2
50	6.8	7.0	6.2

Table 22: pH measurements of cadmium solutions treated with uncoated limestone.

Weight of uncoated limestone (grams)	Post treatment pH			Weight of uncoated limestone used (grams)	Post treatment pH		
	20 ppb Cadmium	40 ppb Cadmium	100 ppb Cadmium		20 ppb Cadmium	40 ppb Cadmium	100 ppb Cadmium
5	7.8	8	7.8	0.1	6.5	6.5	6.1
10	7.9	8.2	7.9	0.2	7.1	6.2	6.5
10	7.9	8.4	7.9	0.2	7	6.6	6.2
20	7.9	8.4	8	0.5	7.5	7.5	6.9
50	8.0	8.4	8.2	1	7.6	7.8	7.3

As can be seen from Tables 21 and 22, the post treatment pH values of all solutions are near neutral. This shows the strong buffering capacity of the limestone. Even small amounts such as 0.1 grams of limestone could buffer 100ml of the metal solutions.

SEM Results

SEM for uncoated limestone

Figures 24 and 25 as well as Table 23 represents the SEM results obtained for limestone before coating.

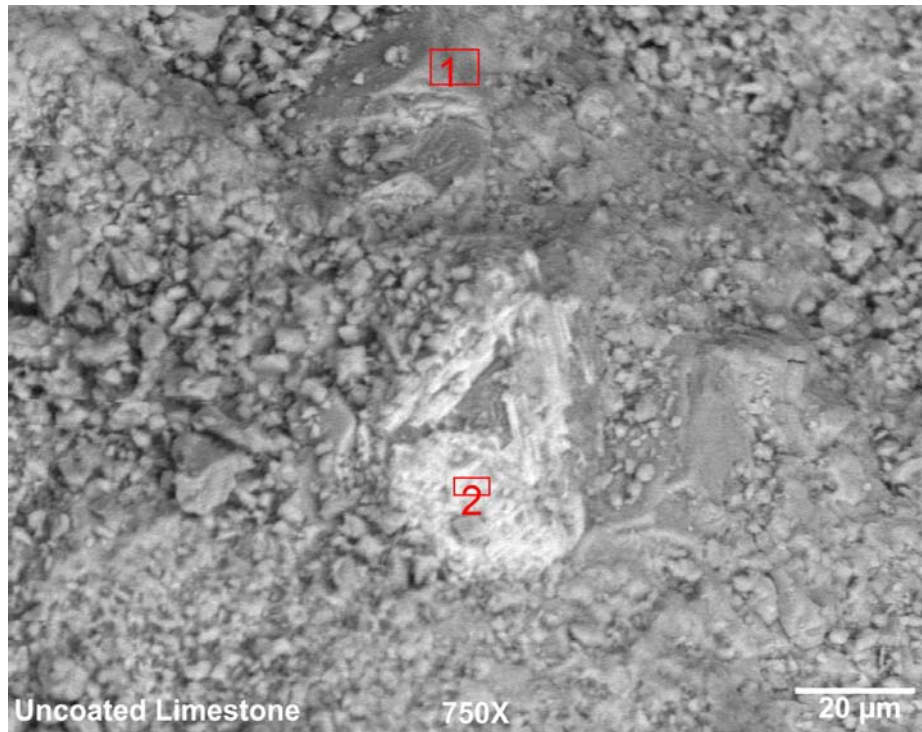


Figure 24: SEM image for uncoated limestone.

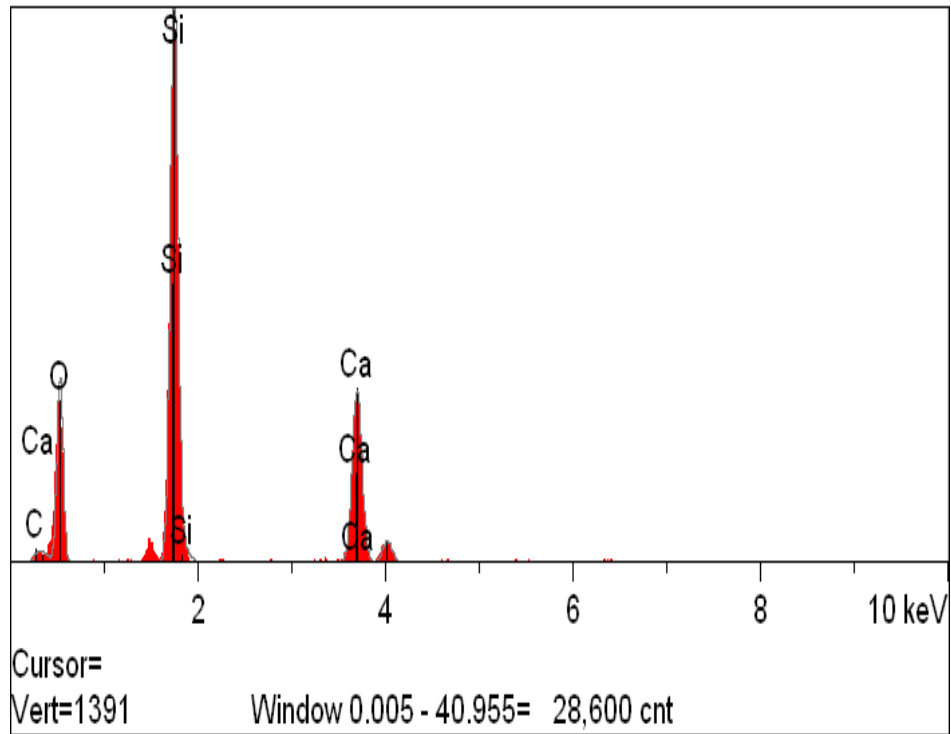


Figure 25: Analysis report for SEM image obtained for uncoated limestone.

Table 23: Analysis data for SEM image obtained for uncoated limestone.

Element	Location 1		Location 2	
	Atomic %	Concentration (wt.%)	Atomic %	Concentration (wt.%)
C	5.07	3.03	9.88	5.71
O	66.35	52.80	66.43	51.13
Si	21.47	30.00	4.38	5.92
Ca	7.11	14.18	19.31	37.24

Figure 25 represents the SEM data obtained for uncoated limestone which shows the surface elements calcium, oxygen, silicon and calcium.

SEM for iron-coated limestone

The acidic effect of iron chloride solutions is clearly seen in Figure 26. The SEM results obtained for limestone after treatment with iron chloride solution are shown in Figures 26 and 27 as well as Table 24.

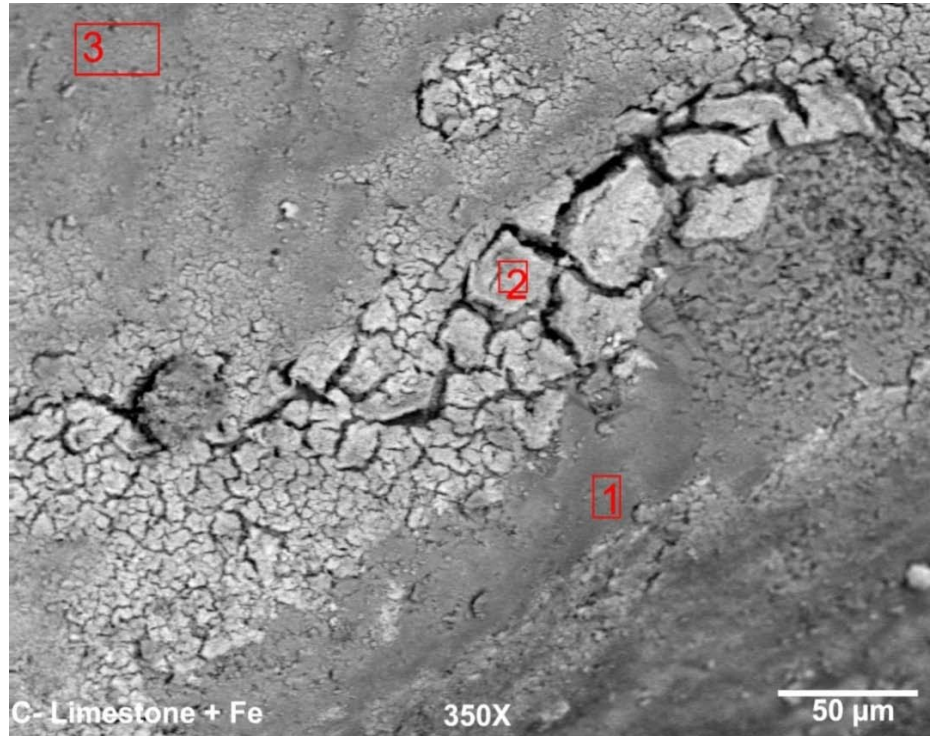


Figure 26: SEM image for iron-coated limestone.

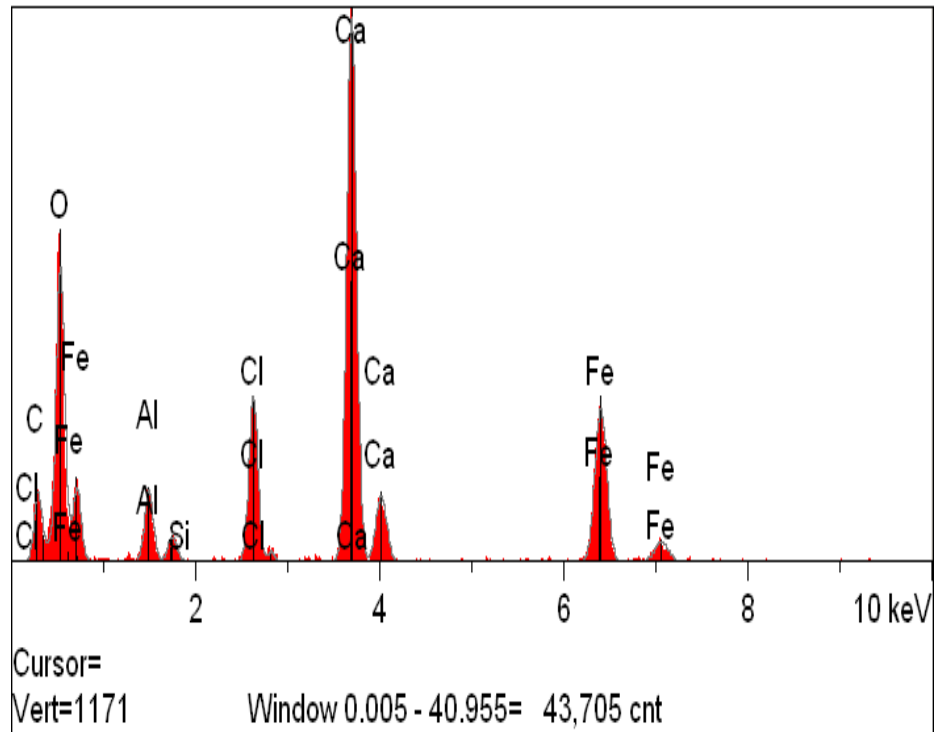


Figure 27: Analysis report for SEM image obtained for iron-coated limestone.

Table 24: Analysis data for SEM image obtained for iron-coated limestone.

Element	Location 1		Location2		Location3	
	Atomic %	Concentration (wt. %)	Atomic %	Concentration (wt. %)	Atomic %	Concentration (wt. %)
C	20.01	13.01	18.17	10.89	16.34	10.23
O	65.46	56.67	63.38	50.58	67.36	56.17
Al	2.95	4.3	1.89	2.55	2.07	2.91
Si	0	0	0.55	0.77	0.29	0.42
Cl	0.47	0.91	2.41	4.27	0.72	1.33
Ca	9.9	21.46	8.8	17.59	11.61	24.24
Fe	1.21	3.65	4.8	13.37	1.61	4.7
Total	100	100	100	100	100	100

Figure 26 represents the SEM data obtained for iron-coated limestone which shows a combination of carbon, oxygen, aluminum, silicon, chlorine, calcium and iron on surface. The images clearly show the uneven distribution of iron on surface confirming the heterogeneous nature of the limestone surface. The major elements were oxygen which constituted about 56 % and around 21% of calcium.

SEM for iron-coated limestone treated with zinc

Images at 350X and 750X were obtained for iron coated limestone coated with zinc were shown in Figures 28 and 29. The SEM data obtained is shown in Figure 30 and Table 25.

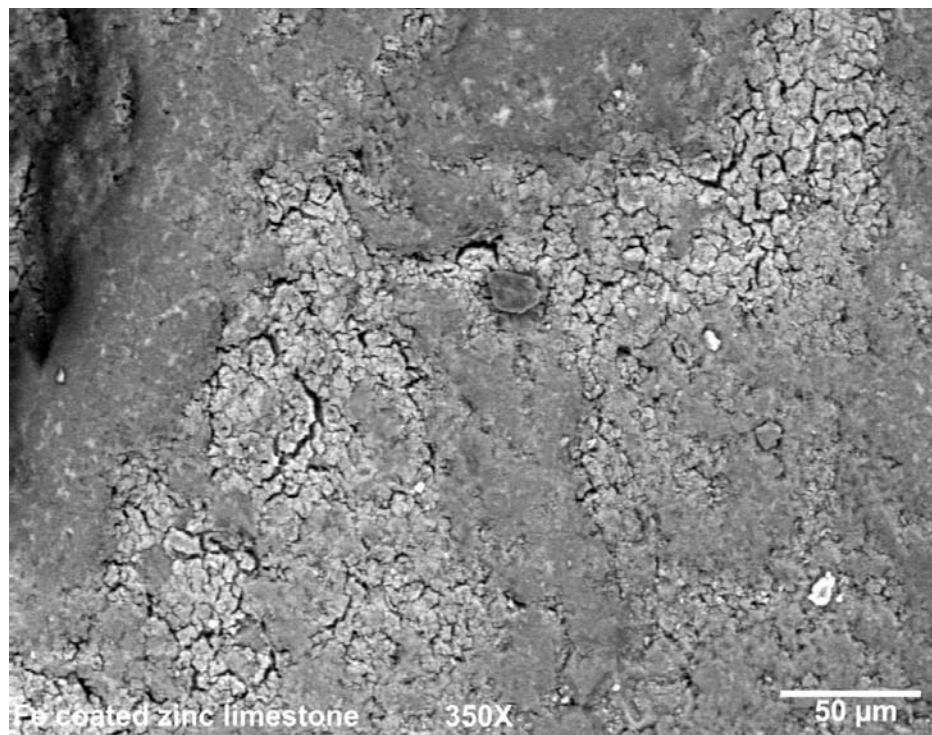


Figure 28: 350X SEM image for iron-coated limestone treated with zinc solution.

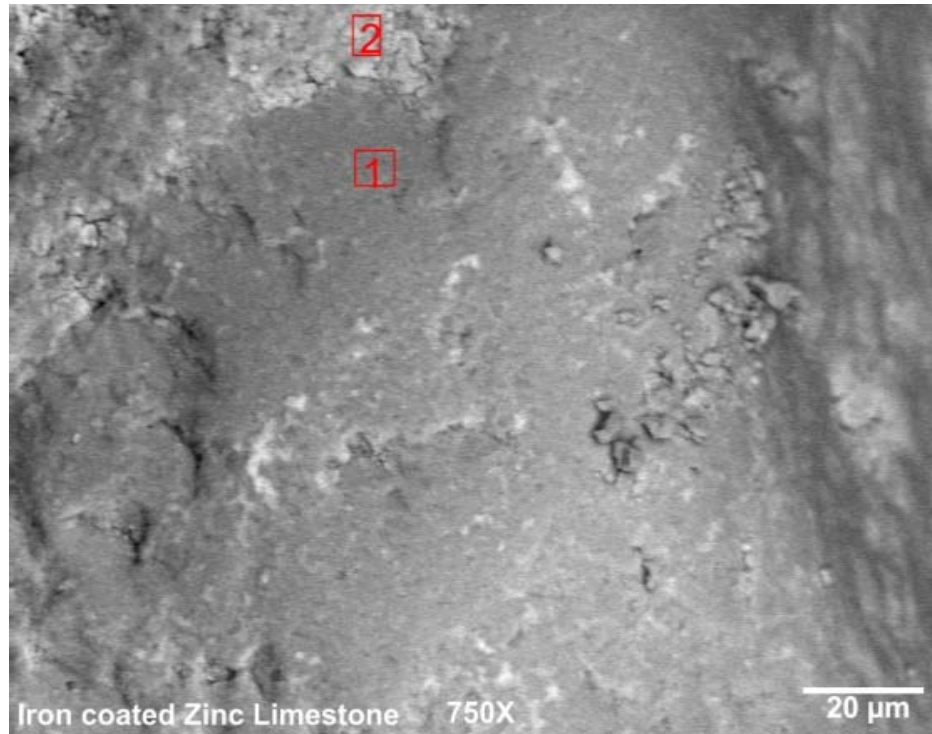


Figure 29: 750X SEM image for iron-coated limestone treated with zinc solution.

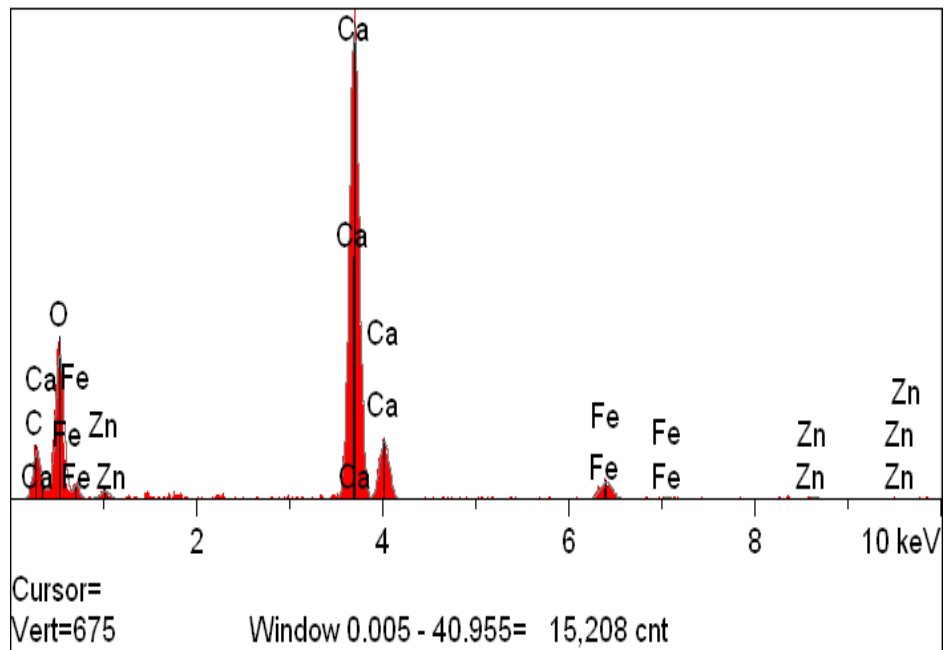


Figure 30: Analysis report for SEM image obtained for iron-coated limestone treated with zinc.

Table 25: Analysis data for SEM image obtained for iron-coated limestone treated with zinc.

Element	Location 1		Location 2	
	Atomic %	Concentration (wt.%)	Atomic %	Concentration (wt.%)
C	14.35	8.96	12.90	7.93
O	70.74	58.82	71.60	58.64
Ca	13.60	28.33	13.63	27.96
Fe	1.10	3.18	1.64	4.69
Zn	0.21	0.70	0.23	0.77

Figure 30 represents the SEM data obtained for iron-coated limestone treated with zinc which showed the presence of carbon, oxygen, calcium, iron and zinc. The image shows the diffuse distribution of the iron. Small amounts of zinc were also seen on the surface.

SEM for uncoated limestone treated with cadmium

The SEM results obtained for uncoated limestone treated with cadmium solution are shown in Figures 31 and 32 as well as Table 26.

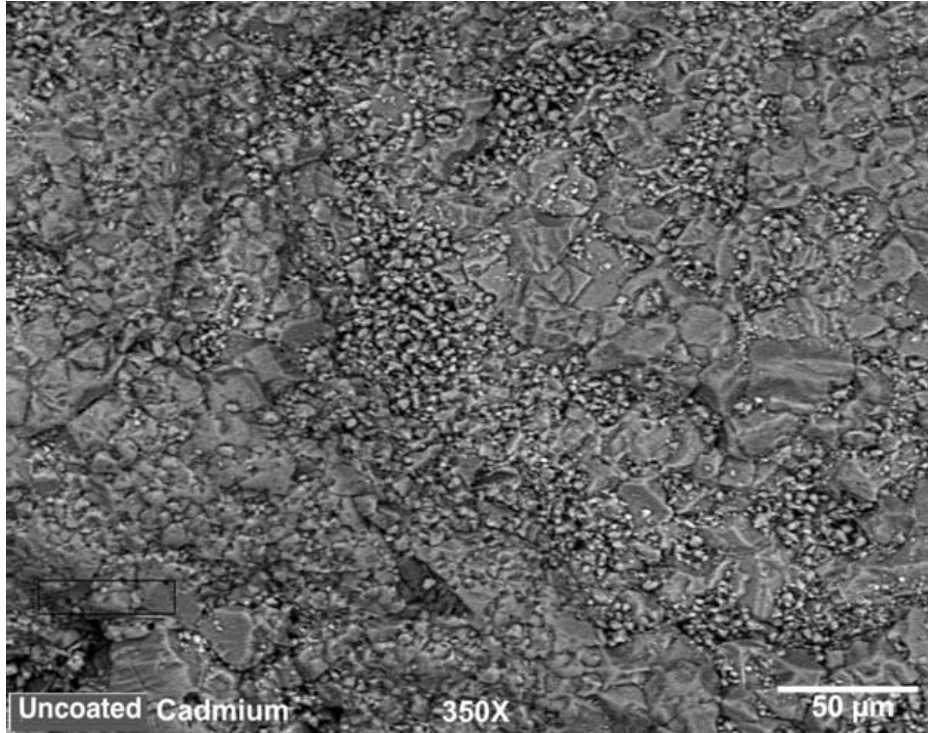


Figure 31: SEM image for uncoated limestone treated with cadmium.

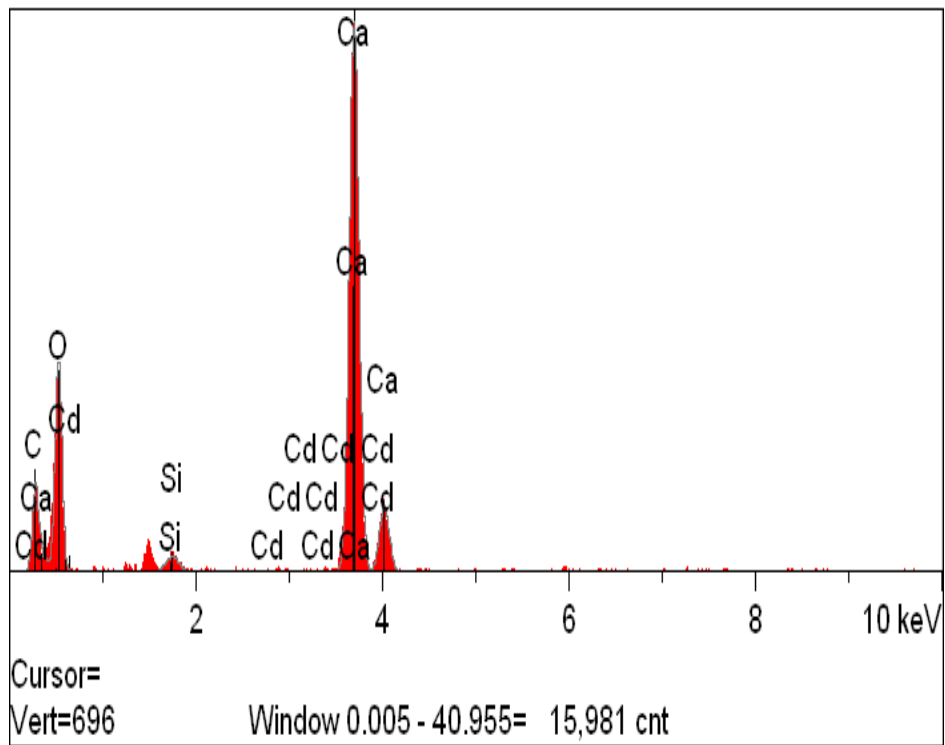


Figure 32: Analysis report for SEM image obtained for uncoated limestone treated with cadmium.

Table 26: Analysis data for SEM image obtained for uncoated limestone treated with cadmium.

Element	Location 1		Location 2	
	Atomic %	Concentration (wt.%)	Atomic %	Concentration (wt.%)
C	16.31	10.57	16.65	10.33
O	70.17	60.59	66.31	54.76
Si	0.68	1.03	0.54	0.79
Ca	12.82	27.73	16.50	34.13
Cd	0.01	0.07	0.00	0.00

Figure 32 and Table 26 represents the SEM data obtained for uncoated limestone treated with cadmium which showed the presence of carbon, oxygen, silicon, calcium and cadmium.

XRD Results

The composition of uncoated limestone and iron coated limestone was studied using XRD. The data obtained was shown in Figure 33 and 34.

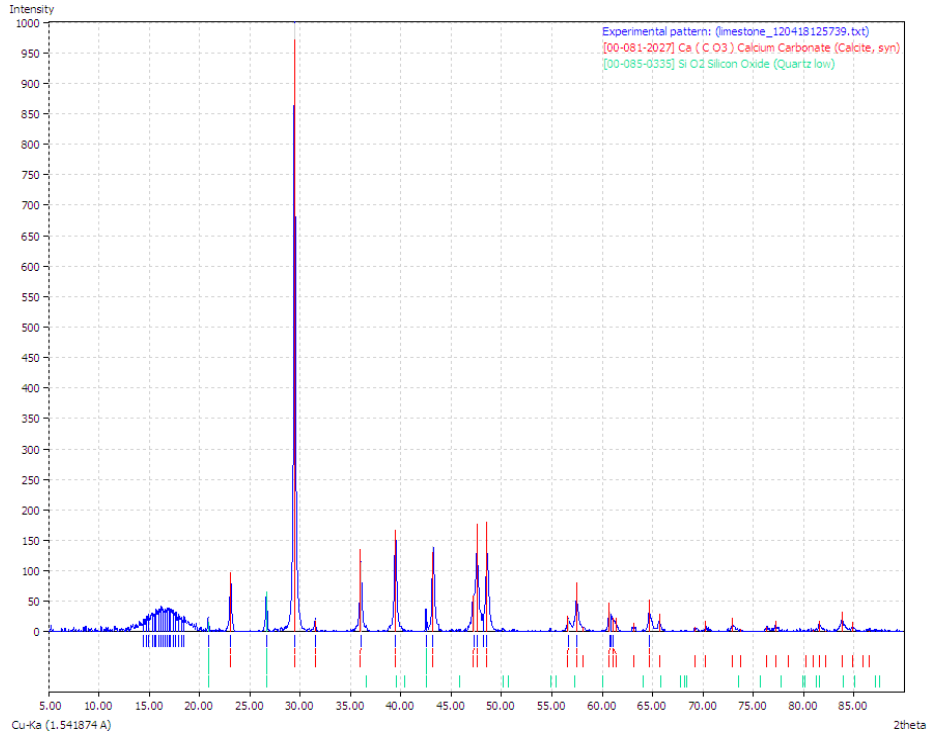


Figure 33: XRD graph comparing peaks of uncoated limestone with calcium carbonate.

Figure 33 represents XRD peaks obtained for uncoated limestone with that of the known compound calcium carbonate. Almost all the peaks matched confirming the base material to be composed of calcium carbonate.

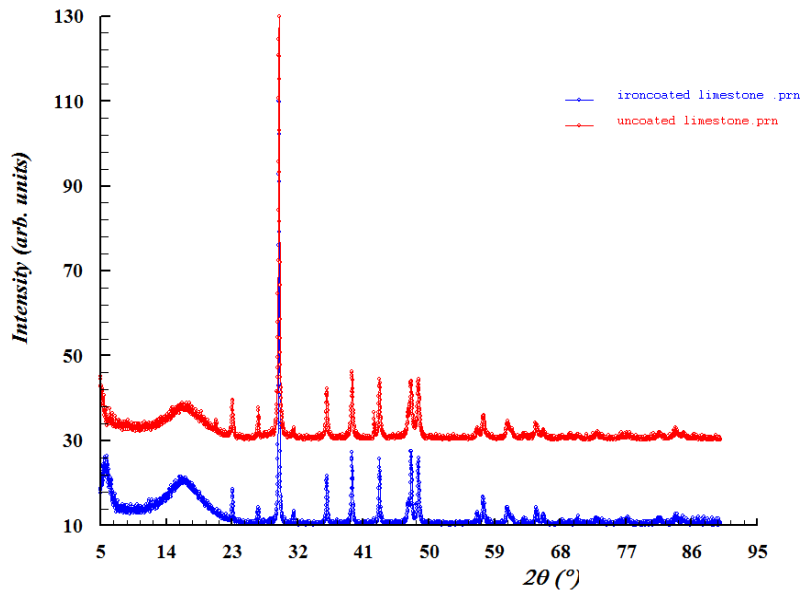


Figure 34: XRD graph comparing uncoated limestone with iron-coated limestone.

Little difference can be seen between the uncoated and iron-coated limestone. Iron hydroxide is amorphous and is finely distributed. It cannot be directly observed at this level using XRD.

Chapter 5

CONCLUSIONS

Heavy metal contamination is a serious worldwide issue faced by many people throughout the world. Groundwater, which is a major source of drinking water, is contaminated with heavy metals by natural as well as human activities, industrial pollution and agricultural pollution. Although several technologies for heavy metal removal have been established, most of them are expensive and complicated. The proposed method uses chicken feed as the base material which is relatively cheap and readily available. Iron coatings enhance the heavy metal removal by increasing the surface area. The effectiveness of the method was studied using kinetics and batch experiments conducted with zinc and cadmium metals. The drinking water standards for zinc and cadmium set by US-EPA are 5 ppm and 5 ppb respectively. This research was mainly focused on reducing the high concentrations of zinc and cadmium to normal drinking water standards by treating with uncoated and iron-coated limestone. Also, the effect of pH on removal efficiency was investigated.

The objective of kinetics experiment was to find the appropriate time required for the maximum removal of the metal. In this study, it was observed that zinc required a minimum of 24 hours for an efficient removal whereas cadmium levels are reduced to zero with both iron-coated and uncoated lime within 15 minutes. Initially kinetics experiment for zinc metal was done using pure limestone without any iron-coatings. The percentage removal of the zinc was only about 50%. The kinetics experiment was repeated using iron-coated limestone and it was observed that iron-coated limestone was more efficient than the pure limestone in removing zinc metal. The removal efficiency

was about 92% for 20 ppm zinc with just 5 grams of iron-coated limestone. Kinetics for cadmium metal was also studied using both iron-coated and plain limestone.

Using these kinetics experiment results, batch tests were performed using zinc metal in iron-coated limestone with an established contact time of 24 hours. All the batch experiments were done using only iron-coated limestone as plain limestone proved to be less effective for zinc removal. Batch tests performed with an initial zinc concentration of 20 ppm, 40 ppm and 100 ppm using varying weights of iron-coated limestone showed maximum removal efficiency at 50 grams which was the highest weight of iron-coated limestone used for all three initial concentrations used. The result showed that iron coated limestone was effective in reducing the zinc concentration to below drinking water standards as seen for all the batches. The pH measured for all the batches after 24 hours of contact time with iron-coated limestone showed an increase from acidic pH of zinc solution to almost a neutral pH range of 6.5-7.5. This is evidence of the limestone's buffering capacity. The effect of pH on removal efficiency studies showed only a slight increase in removal at a pH range of 4-9 which was not significant, indicating pH independence of iron-coated limestone for zinc uptake. Analysis of samples for the detection of iron on ICP-ES showed the presence of 0.001-0.09 ppm levels of iron which was expected to be from the iron coatings on limestone and this means there was very little contamination of iron from the base material. The drinking water standard for iron is 3 ppm.

Batch experiments were performed using cadmium but with plain limestone as it was effective in removing the metal. Batch tests were done with 20 ppb, 40 ppb and 100 ppb cadmium solutions for 2 hours. Nearly 100% removal efficiency was established

with just 5 grams of plain limestone. Further batch experiments were performed to investigate the efficiency of limestone at amounts less than 1 gram and with only 15 minutes contact time. This also showed a removal of 99% from the initial concentration of 20 ppb cadmium metal. A sample of 0.1 gram removed 98.7% of 40 ppb cadmium metal. Though 100% removal was not obtained for second set of batch experiments, the cadmium was reduced well below the drinking water standards. Changing the pH of cadmium standards did not show any significant effect on removal efficiency, all being reduced to below detection limits showing the independence of pH for cadmium removal.

Figures 24 and 26 represent SEM images for plain and iron-coated limestone. The images for iron-coated limestone showed the uneven distribution of iron indicating the heterogeneous nature of the iron coated limestone. Limestone treated with cadmium and zinc showed the presence of the respective metals on the surface confirming their removal. The weight of iron coated limestone was found to be 98.08 grams whereas the initial weight of limestone before the treatment was 100.00 grams accurately. This infers a decrease in the size after treatment with iron chloride solution indicating the dissolution of base material in the acidic pH of iron chloride solution followed by the iron hydroxide precipitation. The XRD studies showed that the uncoated limestone was mostly calcium carbonate. The iron-coated limestone was investigated for the presence of iron hydroxide, iron-carbonate and iron oxide but the peaks obtained were relatively insignificant indicating that the coated substance on surface was very thin and diffusely distributed.

In conclusion, iron-coated limestone proved to be efficient in removing zinc which removed about 99% of the metal whereas plain limestone was efficient in 100% cadmium removal. From the kinetics experiments, it was proved that zinc takes 24 hours for

maximum removal whereas cadmium can be removed within 15 minutes. The pH studies confirmed the pH independence of limestone to remove zinc and cadmium metals. The SEM studies confirmed the heterogeneous nature of limestone surface.

Most of the methods and systems in current use have good efficiency but are technically demanding. We explore a more suitable, inexpensive and efficient method for use in third world nations. The proposed method uses modified limestone which could be readily applied to many natural water systems as it does not produce any toxic products and is readily available.

This is an inexpensive technique which uses chicken feed (limestone) as a base material. Limestone occurs naturally in earth's crust, and acts as the media for heavy metal removal. Saturated material can be easily disposed by mixing with concrete and cement. It can be synthesized and used easily by developing countries. This is a straight forward low-cost process which does not require any complex implementation.

Chapter 6

FUTURE WORK

The efficiency of the limestone to remove other heavy metals in real water samples may also be investigated. Removal efficiency of coated and plain limestone using samples with a mixture of two or more metals could be studied as industrial contamination may sometimes release more than one particular toxic metal. Properties of the zinc and cadmium complexes or precipitates deposited on the limestone can be identified further. Removal efficiency of different types of limestone can be investigated and compared. Other mechanisms involved in heavy metal removal other than adsorption and precipitation could be studied for better applications.

Chapter 7

PERSPECTIVE

Drinking water is polluted with metals that are harmful for people due to waste from industries. There are ways to remove the metals from drinking water but they are hard and costly. We came up with an idea to remove zinc and cadmium with a really simple and cheap material. Our material is limestone. Limestone is available everywhere. Metals are attracted to the surface of limestone and are removed easily. Plain limestone worked well for cadmium but not for zinc. So we just coated the limestone with a small amount of iron, and this removed all the zinc. After the limestone is full, we can just take the limestone back to a cement plant because the metals won't come off.

BIBLIOGRAPHY

- Alexandratos, V. G., Elzinga, E. J. and Reeder, R. J. *Geochim. Cosmochim. Acta.* **2007**, 71, 4172-4187.
- An, H. K., Park, B. Y., Kim, D. S. and *Water Res.* **2001**, 35, 3551-3556.
- Aziz, H. A., Adlan, M. N., Hui, C. S., Zahari, M. S. M. and Hameed, B. H. *Indian J. Eng. Mater. Sci.* **2005**, 12, 248-258.
- Barbosa, A. E. and Hvitved-Jacobsen, T. *Environ. Sci. Technol.* **1999**, 235, 151-159.
- Benner, T. C. *Environ. Sci. Technol.* **2004**, 38, 3457-3464.
- Brookins, D. G. *Eh-Ph Diagrams for Geochemistry*, Springer-Verlog, New York, **1988**, 176p.
- Callender, E. and Rice, K. C. *Environ. Sci. Technol.* **2000**, 34, 232-238.
- Carlson, L., Bigham, J. M., Schwertmann, U., Kyek, A., and Wagner, F. *Environ. Sci. Technol.* **2002**, 36, 1712-1719.
- Carroll, S. A., Oday, P. A. and Piechowski, M. *Environ. Sci. Technol.* **1998**, 32, 956-965.
- Chen, J. p. and Yu, H. J. *Environ. Sci. Health.* **2000**, 35, 817-835.
- Cotton, F. A., Wilkinson, G., Murillo, C. A. and Bochmann, M. *Advanced Inorganic Chemistry*, 6th Edition, **1999**, 598-629.
- Councill, T. B., Duckenfield, K. U., Landa, E. R., and Callender, E. *Environ. Sci. Technol.* **2004**, 38, 4206-4214.
- Dannis, M. L. *Rubber Chem. Technol.* **1974**, 47, 1011-1037.
- Darwish, I. A. and Blake, D. A. *Anal. Chem.* **2001**, 73, 1889-1895.
- Dhananjay, M. and James, F. J. *Environ. Sci. Technol.* **2005**, 39, 9689-9694.
- Duckworth, O. W. and Martin, S. T. *American Minerologist.* **2004**, 89, 554-563.

- Ferguson, M. A., Fernandez, D. P. and Hering, J. G. *J. American Water Works Association*. **2007**, 99, 92-98.
- Flegler, S. L., Heehman, J. W. and Klomparens, K. L. *Scanning and Transmission Electron Microscopy An Introduction*.
- Gardea-Torresdey, J. L., De La Rosa, G. and Peralta-Videa, J. R. *Pure Appl. Chem.* **2004**, 76, 801-813.
- Gu, Z., Jun, F., and Baolin, D. *J. Environ. Sci. Technol.* **2005**, 39, 3833-3843.
- Hildemann, L. M., Markowski, G. R.; Cass. G. R. *Environ. Sci. Technol.* **1991**, 25, 744-759.
- Hossain, M. A., Sengupta, M. K., Ahamed, S., Rahman, M. M., Mondal, D., Lodh, D., Das, B., Nayak, B., Roy, B., Mukherjee, A. and Chakraborti, D. *Environ. Sci. Technol.* **2005**, 39, 4300-4306.
- Janet, G. H., Pen-Yuan, C., Jennifer, A. W. and Menachem, E. *J. of Environ. Eng.* **1997**, 800-807.
- Kim, M. J., Nriagu, J. and Haack, J. *J. Environ. Sci. Technol.* **2000**, 34, 3094-3100.
- Klimmek, S., Stan, H. J., Wilke, A., Bunke, G. and Buchholz, R. *Environ. Sci. Technol.* **2001**, 35, 4283-4288.
- Kohler, S. J., Cubillas, P., Blanco, J. D. R., Bauer, C. and Prieto, M. *Environ. Sci. Technol.* **2007**, 41, 112-118.
- Le, X. C., Yalcin, S. and Ma, M. *J. Am. Chem. Soc.* **2000**, 34, 2342-2347.
- Lee, M. H., Cho, K., Shah, A. P., and Biswas, P. *Environ. Sci. Technol.* **2005**, 39, 8481-8489.
- Legret, M. and Pagotto, C., *Sci. Tot. Environ.* **1999**, 235, 143-150.

- Mause, Y., Loppert, R. H. and Kramer, T. A. *Environ. Sci. Technol.* **2007**, 41, 837-842.
- Nurul, A., Satoshi, K., Taichi, K., Aleya, B., Hideyuki, K., Tohru, S. and Kiyohisa, O. *Ind. Eng. Chem. Res.* **2006**, 45, 8105-8110.
- Pal, P., Sarkar, P. and Bhattacharyay, D. *Sensor Letters.* **2010**, 8, 577-583.
- Peters, S. C., Blum, J. D, Klauke, B. and Karagas, M. R. *Environ. Sci. Technol.* **1999**, 33, 1328-1333.
- Pierson, W. R. and Brachaczek, W. W. *Rubber Chem. Technol.* **1974**, 47, 1275-1299.
- Romero, F. M., Armienta, M. A. and Carrillo-Chavez, A. *J. Arch. Enviorn. Contam. Toxicol.* **2004**, 47, 1-13.
- Silva, A. M., Cruz, F. L. S., Lima, R. M. F., Teixeira. and M. C., Leao, V. A. *J. of Hazardous Materials.* **2010**, 181, 514-520.
- Stocker, J., Balluch, D., Monika, G., Harms, H., Feliciano, J., Daunert, S., Malik, K. A. and Meer, J. R. V. D. *Environ. Sci. Technol.* **2003**, 37, 4743-4750.
- Skoog, Holler, and Nieman, *Principles of Instrumental Analysis.* 5th Edition, **1998**, 230-250.
- Tani, C., Inoue, K., Tani, Y., Harun-Ur-Rashid, Md., Azuma, N., Ueda, S., Yoshida, K. and Maeda, I. *J. Bioscience and Bioengineering.* **2009**, 108, 414-420.
- Turner, B. D., Binning, P. and Stipp, S. L. S. *Environ. Sci. Technol.* **2005**, 39, 9561-9568.
- Yoko, M., Richard, L. H., and Tim, K. A. *J. Environ. Sci. Technol.* **2007**, 41, 837-842.
- Yu, D., Wu, F. and Cao, A. Method for Detecting Arsenic content by Iodine Solution Absorption. *Faming Zhunali Shenqing.* **2010**.
- Yuan, D. and Liu, J. *Zhongguo Redai Yixue.* **2010**, 10, 389-390.

- Zereini, F., Alt, F., Messerschmidt, J., Wiseman, C., Feldmann, I., Bohlen, A. V., Muller, J., Liebl, K. and Puttmann, W. *Environ. Sci. Technol.* **2005**, 39, 2983-2989.
- Zhang, Q., Pan, B., Pan, B., Zhang, W., Jia, K. and Zhang, Q. *Environ. Sci. Technol.* **2008**, 42, 4140-4145.
- Zhigang, Y., Lifa, Z., Zhengyu, B., Pu, Gao. and Xingwang, S. *J. Geochem.* **2009**, 28, 293-298.
- Zhou, P., Huang, J. C., Li, A. and Wei, S. *Water Res.* **1993**, 33, 1918-1924.

